

A GENERAL THEORY FOR THE ACCURATE STRESS ANALYSIS OF HOMOGENEOUS AND LAMINATED COMPOSITE BEAMS

KOSTAS P. SOLDATOS and PHILIP WATSON

Department of Theoretical Mechanics, University of Nottingham, Nottingham
NG7 2RD, U.K.

(Received 17 November 1995; in revised form 25 July 1996)

Abstract—This paper has a twofold purpose. Initially, it presents a general four-degrees-of-freedom beam theory (G4DOFBT) which takes into consideration the effects of both transverse shear and normal deformation. On the basis of this new theory, it then proposes a method suitable for the accurate stress analysis of either homogeneous or laminated composite beams subjected to arbitrary edge boundary conditions. The new beam theory involves two general “shape” functions, each of which is associated with one of the two unknown displacement components. Upon assigning simple particular forms to these shape functions, most of the well-known classical and variationally consistent refined beam models may be obtained as particular cases. The new method for the accurate stress analysis of beam-type structures is based on the specification of a new pair of shape functions. These are obtained by introducing the stress distributions, caused by the assumed G4DOFBT displacement field, into the appropriate equations of three-dimensional elasticity which are subsequently solved for simply supported edges. This is considered to provide an excellent choice of both shape functions as the method then yields the exact elasticity solution presented by Pagano (Pagano, N. J. (1969). Exact solution for composite laminates in cylindrical bending. *J. Comp. Mat.* 3, 398–411) for the cylindrical bending problem of simply supported infinite strips. Two particular examples are considered to show the potential of the present analysis. These are dealing with stress analysis of homogeneous or laminated composite beams having one edge rigidly clamped and the other edge either guided or free of external tractions. © 1997 Elsevier Science Ltd.

1. INTRODUCTION

The rapid increase in the industrial use of advanced composite materials has necessitated the development of refined theories suitable for the analysis and study of the mechanical behaviour of composite thin-walled structures. These refined theories take the effects of transverse deformation into consideration making them useful in the static or dynamic analyses of homogeneous and laminated highly reinforced composite beams, plates and shells. Dealing in particular with laminated composite beam-type structures, one has to abandon the classical Euler–Bernoulli assumptions.

The simplest possible refined laminated beam theory is obtained by extending the Timoshenko (1922) beam model, which neglects transverse normal deformation and assumes a linear through-thickness variation of shear strain, to the configuration of a laminated composite material. Due to the bending–extension coupling of a laminate, such a refinement yields three coupled ordinary differential equations for the three generalised displacement unknowns (degrees of freedom), namely the axial and transverse displacements and the rotation of the beam central axis. An even more advanced beam model can be obtained by similarly extending the Bickford (1982) beam model. This still neglects transverse normal deformation but assumes a parabolic through-thickness variation of shear strain. Although it violates shear stress continuity at the material interfaces of a laminated beam, such a beam model makes no use of a shear correction factor, it still employs only three independent generalised displacement components (this is considered to be the smallest possible number of degrees of freedom for a shear deformable beam theory).

Refined laminated beam models accounting for interlaminar continuity of both displacements and shear stress have already appeared in the literature (Di Taranto, 1973; Rao, 1976, 1977, 1978; Heuer, 1992). The applicability of the theories presented in literature

(Di Taranto, 1973; Rao, 1976; Heuer, 1992) is confined to beams composed of only three layers, while Rao's (1977, 1978) model treats each particular layer of an N -layered beam as a separate Timoshenko beam, finally resulting in $N+2$ degrees of freedom. Moreover, appropriate one-dimensional versions of relevant shear deformable plate models (Di Sciuva, 1986; Lee *et al.*, 1990; Savithri and Varadan, 1990; Cho and Parmeter, 1992; Soldatos, 1992a; Touratier, 1992) produce other refined beam theories at various levels of sophistication all of which still only use three degrees of freedom.

All of the aforementioned refined beam and plate theories assume that the transverse shear deformation is distributed in the form of a lower order polynomial of the transverse co-ordinate, z (some of the coefficients of which may appropriately depend on the transverse elastic moduli), or in the form of a certain elementary function of z (trigonometric or hyperbolic). Hence, they all suffer from the main stress-analysis drawback of all conventional one-dimensional beam models and two-dimensional plate and shell theories; they cannot accurately predict the well-known boundary layer behaviour of in-plane stress and displacement distributions either near the material interfaces of a laminate or near the lateral planes of a highly reinforced structural element.

The main reason for this drawback becomes evident when observing the form of relevant exact three-dimensional elasticity solutions (Pagano, 1969; Srinivas and Rao, 1970; Ye and Soldatos, 1994a, b). All of these solutions suggest that the through-thickness distributions of the in-plane displacements and stresses vary in an exponential rather than in a polynomial form and that in-plane elastic moduli always appear in the exponents involved. With these moduli being assigned substantially high values in the case of highly reinforced materials, the in-plane stresses and displacements take high values away from the central surface ($z = 0$), therefore giving rise to the above boundary layer behaviour of the corresponding distributions. Another reason for the stress-analysis inaccuracy of conventional refined beam, plate and shell theories may be the common omission of the transverse normal deformation. Although this omission is usually considered to cause only a small loss of accuracy in the relevant stress analysis, laminated thin-walled structures are sensitive to transverse normal deformation. Also, the transverse normal deformation contributes to the transverse normal and shear stresses which are thought to be responsible for delamination failure of composites.

Hence, this paper has a twofold purpose. Initially, it presents a general four-degrees-of-freedom beam theory (G4DOFBT) which takes into consideration the effects of both transverse shear and normal deformation. On the basis of this new theory, it then proposes a method suitable for the accurate stress analysis of either homogeneous or laminated composite beams. In a close relation to a series of recent publications (Soldatos 1992a-c, 1993a, b, 1995; Soldatos and Timarci, 1993), G4DOFBT involves two general "shape" functions, each one of which is associated with one of the two unknown displacement components. The equations of equilibrium of G4DOFBT are obtained by means of the new vectorial approach presented in Soldatos (1995). Upon assigning simple particular forms to these shape functions, most of the well-known classical and variationally consistent refined beam models can be obtained as particular cases of G4DOFBT. Moreover, further possibilities have been left open, in the sense that a more appropriate *a-posteriori* specification of the shape functions might well result in an improvement of the performance of G4DOFBT without altering its theoretical formulation.

The new method for the accurate stress analysis of beam-type structures is based on the specification of a new pair of shape functions. These are obtained by introducing the stress distributions, caused by the assumed G4DOFBT displacement field, into the appropriate equations of three-dimensional elasticity which are subsequently solved for simply supported edges. This is considered to provide an excellent choice of both shape functions as the method then yields the exact elasticity solution presented by Pagano (1969) for the cylindrical bending problem of simply supported infinite strips. The importance of the present analysis lies on the grounds of its potential in dealing with the accurate stress analysis of homogeneous or laminated composite beams subjected to more realistic sets of edge boundary conditions. To show this, two relatively simple examples are considered, both of which deal with displacement and stress distributions within homogeneous and

two-layered laminated beams. In both cases the left edge of the beam is assumed to be rigidly clamped while its right edge is taken to be free of tractions in the first example and guided in the second.

2. THE GENERAL FOUR-DEGREES-OF-FREEDOM BEAM THEORY (G4DOFBT)

Consider a straight elastic beam, the central axis of which coincides with the Ox -axis of a Cartesian co-ordinate system $Oxyz$ (the positive Oz axis is directed upwards). The length and thickness of the beam are denoted by L and h , respectively, while it is assumed, for simplicity, that its width is unity. With this latter simplification, the theory can be applied or extended to the static and dynamic analyses of beams of general compact cross-sections (see, for instance, Donnell, 1976). The beam is composed of an arbitrary number, N of orthotropic linearly elastic layers whose planes of material symmetry coincide with the co-ordinate planes.

It is further assumed that the beam is subjected to an external transverse load, q , acting normally and downwards on the top lateral plane and distributed symmetrically with respect to the co-ordinate plane Oxz . Hence, displacements are principally in this plane (zero displacement component across the Oy direction) and q is essentially considered to be a known function of x only. All quantities involved are independent of the co-ordinate parameter y and the beam is therefore assumed to be under plane strain deformation in the co-ordinate plane Oxz . Under these considerations, the second equilibrium equation of three-dimensional elasticity is satisfied identically. Hence, in what follows, the term "three-dimensional elasticity" should be taken to mean "exact two-dimensional plane strain elasticity".

For the static analysis of that beam, the formulation of the G4DOFBT begins with the displacement model:

$$\begin{aligned} U(x, y, z) &= U^c(x, y, z) + U^a(x, y, z), \\ W(x, y, z) &= W^c(x, y, z) + W^a(x, y, z), \end{aligned} \quad (1)$$

where U and W represent displacement components along the x and z directions, respectively. This is a superposition of two different displacement fields. The basic displacement field,

$$\begin{aligned} U^c(x, y, z) &= u(x, y) - zw_{,x}, \\ W^c(x, y, z) &= w(x, y), \end{aligned} \quad (2)$$

is the displacement approximation employed in the development of classical beam theory, while the additional field,

$$\begin{aligned} U^a(x, y, z) &= \varphi(z)u_1(x, y), \\ W^a(x, y, z) &= \psi(z)w_1(x, y), \end{aligned} \quad (3)$$

dismisses the Euler–Bernoulli assumptions and incorporates the effects of transverse shear and normal deformation.

The functions $\varphi(z)$ and $\psi(z)$ are assumed to be given functions of the transverse co-ordinate parameter and, by means of their derivatives [see eqns (5) and (6) below], they dictate the "shape" of the transverse deformation effects. These functions may be chosen in several different ways, most of which yield approximate through-thickness displacement and stress distributions. Further comments of such realistic but approximate possible choices of $\varphi(z)$ and $\psi(z)$ are given later in this section, while a method which provides their exact form, for simply supported beams, is presented in Section 4. At this stage, however, no particular forms are assigned to these functions. For notational convenience it is assumed

that they both have the dimensions of length. Moreover, by enforcing u and w to represent the displacements of the beam central axis (see, for instance, Timoshenko, 1922; Donnell, 1976) and u_1 and w_1 to be the values of the transverse strains on the central axis, further constraints might be imposed on $\varphi(z)$ and $\psi(z)$. Although these are only potential requirements, and as such might be ignored, the former impose the following constraints on $\varphi(z)$ and $\psi(z)$:

$$\varphi(0) = \psi(0) = 0, \quad (4a)$$

while the later impose the following constraints on their derivatives [see eqns (5) and (6) below]:

$$\left. \frac{d\varphi}{dz} \right|_{z=0} = \left. \frac{d\psi}{dz} \right|_{z=0} = 1. \quad (4b)$$

Upon applying the kinematic relations of three-dimensional elasticity on the displacement approximation (1)–(3), one obtains the following non-zero strain components:

$$\varepsilon_x = e_x^c + zk_x^c + \varphi(z)k_x^a, \quad \gamma_{xz} = \varphi'(z)e_{xz}^a + \psi(z)k_{xz}^a, \quad \varepsilon_z = \psi'(z)e_z^a, \quad (5)$$

where a prime denotes ordinary differentiation, with respect to z , and,

$$e_x^c = u_x, \quad k_x^c = -w_{xx}, \quad e_{xz}^a = u_1, \quad e_z^a = w_1, \quad k_x^a = u_{1,x}, \quad k_{xz}^a = w_{1,x}. \quad (6)$$

In these expressions, a kernel letter e denotes strain quantities, while a kernel letter k denotes curvature quantities.

Evidently, two kinds of non-zero central axis strain component occur. The single one denoted by a superscript “ c ”, e_x^c , is identical with its Euler–Bernoulli beam theory counterpart. The additional ones are purely due to transverse shear and normal deformation effects and are denoted by a superscript “ a ”; after eqns (4), they take the values of the transverse strains, ε_z and γ_{xz} , on the beam central axis. In this respect, it now becomes clear that $\psi(z)$ together with the derivative of $\varphi(z)$ dictate the “shape” of the transverse shear strains, while $\psi'(z)$ dictates the “shape” of the transverse normal strain across the beam thickness. Finally, two kinds of central axis curvature and twist occur; the one denoted with a superscript “ c ” is again identical with its classical beam theory counterpart whereas the additional ones are also due to purely transverse shear and normal deformation effects.

Upon denoting \hat{W} to be the strain energy density of the elastic beam considered, the approximate stress field associated to the above approximations is represented by introducing the generalised stress components,

$$\sigma_x^c = \frac{\partial \hat{W}}{\partial e_x^c}, \quad \tau_{xz}^a = \frac{\partial \hat{W}}{\partial e_{xz}^a}, \quad \sigma_z^a = \frac{\partial \hat{W}}{\partial e_z^a}, \quad (7)$$

together with the following generalised moment components:

$$m_x^c = \frac{\partial \hat{W}}{\partial k_x^c}, \quad m_{xz}^a = \frac{\partial \hat{W}}{\partial k_{xz}^a}, \quad m_x^a = \frac{\partial \hat{W}}{\partial k_x^a}. \quad (8)$$

On the basis of these definitions and using the chain rule of partial differentiation (Soldatos, 1992a–c, 1993a, b, 1995), one obtains firstly the conventional force and moment resultants,

$$(N_x^c, M_x^c) = \int_{-h/2}^{h/2} \sigma_x(1, z) dz, \quad (9)$$

employed in the classical beam theory, and secondly the following additional force and moment resultants:

$$(Q_x^a, M_x^a) = \int_{-h/2}^{h/2} (\tau_{xz}\varphi'(z), \sigma_x\varphi(z)) dz, \quad (N_z^a, P_x^a) = \int_{-h/2}^{h/2} (\sigma_z\psi'(z), \tau_{xz}\psi(z)) dz. \quad (10)$$

It is of interest to note, at this point, that upon setting $\varphi(z) = \psi(z) = 0$ all of the additional force and moment resultants are cancelled, leaving only the conventional force and moment resultants (9) employed in classical beam theory. This further clarifies that all additional force and moment resultants (10) are due to the incorporation of transverse deformation effects. Thus, the appearance of two distinguished sets of force and moment resultants agrees completely with the formulation of the displacement approximation (1) as a superposition of two corresponding displacement fields. The basic set (9) of conventional force and moment resultants matches the basic displacement field (2) employed for the development of classical beam theory. On the other hand, the additional set (10) of non-conventional (or *higher-order*) force and moment resultants fits very well with the additional displacement field (3) which dismissed the Euler–Bernoulli assumptions and introduced the effects of transverse deformation.

It is of further interest to note that upon employing $\psi(z) = 0$, but assuming a non-zero form for $\varphi(z)$, transverse normal deformation is neglected. This is one of the most common choices in modelling the mechanical behaviour of homogeneous and composite beams using one-dimensional theories. It reflects the fact that the transverse normal deformation is of a higher-order of magnitude compared to the transverse shear deformation effects and, therefore, only three degrees of freedom are involved (u, w and u_1). In such a case, the higher-order resultants defined in eqn (10b) are dropped. A careful inspection of the right-hand-sides of eqns (10a) reveals that for a linear choice of the remaining shape function, $\varphi(z) = z$, all remaining additional force and moment resultants, which are due to the transverse shear deformation effects, reduce to the form of the corresponding conventional resultants employed in the Timoshenko (1922) beam model. Hence, no controversies occur between the above definitions (9) and (10) and the intuitive definitions of conventional force and moment resultants. Upon employing non-linear forms to the shape function $\varphi(z)$ (see, for instance, Bickford, 1982) the conventional shear force resultants disappear and are replaced with the corresponding *non-conventional* resultants defined according to eqns (10a).

Hence, any non-zero choice of $\psi(z)$ may be considered as giving rise to a second part of the additional strain state incorporating the effects of transverse normal deformation. These are represented by the fourth degree of freedom, w_1 , and further give rise to a corresponding stress state represented by the higher-order force and moment resultants defined in eqn (10b).

The four equations of equilibrium of G4DOFBT can be obtained either variationally or vectorially. The first part of the refined vectorial approach presented in (Soldatos, 1993a, 1995) essentially coincides with the conventional vectorial approach. It involves appropriate integrations of the three-dimensional equations of equilibrium and, after the afore-

mentioned plane strain assumptions, yields the following one-dimensional equations,

$$N_{x,x}^c = 0, \quad M_{x,xx}^c = q(x). \quad (11a, b)$$

Each one of these equations is identical to its corresponding classical beam theory counterpart. Hence, the first part of the vectorial approach deals with balancing conventional force and moment resultants, the appearance of which is consistent with the Euler–Bernoulli assumptions.

The second part of the refined vectorial approach deals with the balancing of the force and moment resultants due to the transverse deformation effects. Accordingly, the first and third of the three-dimensional equations of equilibrium are multiplied by $\varphi(z)$ and $\psi(z)$, respectively, and are then integrated through the plate thickness to yield,

$$M_{x,x}^a - Q_x^a = 0, \quad P_{x,x}^a - N_z^a = \psi(h/2)q(x). \quad (11c, d)$$

It should be mentioned that there is a remarkable similarity between eqn (11c) and its corresponding uniform shear deformable beam theory counterpart (Timoshenko, 1922). The only difference is that additional force and moment resultants have replaced the corresponding conventional quantities. The fourth equilibrium eqn (11d) occurs naturally as the last equation needed to balance all effects caused by the aforementioned second part of additional strain state, which incorporated transverse normal deformation effects into the present theory.

The equations of equilibrium (11) are accompanied by several variationally admissible sets of edge boundary conditions. These can be obtained, naturally, only on the basis of a variational approach. For the most general form of plate displacement expansions, these have been presented in (Soldatos, 1995), the displacement model (1)–(3) being a particular case. Hence, all such sets of boundary conditions applicable to the edges $x = 0, L$ are given as follows:

$$\begin{aligned} &u \text{ prescribed or } N_x^c \text{ prescribed,} \\ &w \text{ prescribed or } M_{x,x}^c \text{ prescribed,} \\ &w_{,x} \text{ prescribed or } M_x^c \text{ prescribed,} \\ &u_1 \text{ prescribed or } M_x^a \text{ prescribed,} \\ &w_1 \text{ prescribed or } P_x^a \text{ prescribed.} \end{aligned} \quad (12)$$

3. FLEXURE OF SIMPLY SUPPORTED ORTHOTROPIC LAMINATED BEAMS

Consider the aforementioned straight beam which is composed of an arbitrary number, N , of perfectly bonded orthotropic layers. The generalised Hooke's law in the r th layer of such a cross-ply laminate is given as follows (Jones, 1975):

$$\begin{Bmatrix} \sigma_x^{(r)} \\ \sigma_z^{(r)} \end{Bmatrix} = \begin{bmatrix} C_{11}^{(r)} & C_{13}^{(r)} \\ C_{13}^{(r)} & C_{33}^{(r)} \end{bmatrix} \begin{Bmatrix} \epsilon_x^{(r)} \\ \epsilon_z^{(r)} \end{Bmatrix}, \quad \tau_{xz}^{(r)} = C_{55}^{(r)} \gamma_{xz}^{(r)}. \quad (13)$$

It should be emphasised that, unlike the corresponding definitions used in all conventional laminate plate and beam theories where the layer superscript (r) is associated with the stresses and the elastic constants only, here a superscript (r) is further associated with all strain components. This is due to the fact that, as shown in the next section, the set of appropriate shape functions $\varphi(z)$ and $\psi(z)$ employed in this paper depends on the elastic constants and, therefore, on the material properties of the r th layer. It should be understood, however, that in the case of a conventional laminated beam theory, in which all shape functions are assumed to be simple polynomials of the transverse co-ordinate parameter,

the layer superscript appearing in the strain components should be ignored. Similarly, all superscripts that appear in eqns (13) should be ignored for the particular case of a homogeneous orthotropic plate, which is represented by the choice $N = 1$.

With the use of eqns (5), (6), (13), (9) and (10), eqns (11) yield the following set of four Navier-type differential equations :

$$\begin{aligned}
 A_{11}^c u_{,xx} - B_{11}^c w_{,xxx} + B_{11}^a u_{1,xx} + B_{13}^b w_{1,x} &= 0, \\
 B_{11}^c u_{,xxx} - D_{11}^c w_{,xxxx} + D_{11}^a u_{1,xxx} + D_{13}^b w_{1,xx} &= q, \\
 B_{11}^a u_{,xx} - D_{11}^a w_{,xxx} + D_{11}^{aa} u_{1,xx} - A_{55}^{aa} u_1 + (D_{13}^{ab} - A_{55}^{ab}) w_{1,x} &= 0, \\
 -B_{13}^b u_{,x} + D_{13}^b w_{,xx} - (D_{13}^{ab} - A_{55}^{ab}) u_{1,x} + A_{55}^{bb} w_{1,xx} - D_{33}^{bb} w_1 &= \psi(h_{N+1})q, \tag{14}
 \end{aligned}$$

for the four main unknown displacement functions: u , w , u_1 and w_1 . Here, the appearing rigidities are given as follows :

$$\begin{aligned}
 (A_{11}^c, B_{11}^c, D_{11}^c, B_{11}^a, D_{11}^a, D_{11}^{aa}) &= \int_{-h/2}^{h/2} C_{11}^{(r)}(1, z, z^2, \varphi, z\varphi, \varphi^2) dz, \\
 (B_{13}^b, D_{13}^b, D_{13}^{ab}) &= \int_{-h/2}^{h/2} C_{13}^{(r)}(\psi', z\psi', \varphi\psi') dz, \\
 (A_{55}^{aa}, A_{55}^{ab}, A_{55}^{bb}) &= \int_{-h/2}^{h/2} C_{55}^{(r)}((\varphi')^2, \varphi'\psi, \psi^2) dz, \quad D_{33}^{bb} = \int_{h/2}^{h/2} C_{33}^{(r)}(\psi')^2 dz. \tag{15}
 \end{aligned}$$

In accordance with the number of edge boundary conditions (12), eqns (14) form a tenth order set of ordinary differential equations, with respect to the axial co-ordinate parameter x . Among the many different combinations of edge boundary conditions that eqns (12) can produce, only one particular set is usually chosen to model the situation that arises in a corresponding application. Nevertheless, such a set of one-dimensional edge boundary conditions always has a three-dimensional elasticity analogue represented by only two boundary conditions applied point by point at each edge, through the beam thickness. This reduced number of the corresponding three-dimensional edge boundary conditions is obviously a reflection of the fact that the two remaining Navier equations of plane strain elasticity form a fourth-order set of partial differential equations, with respect to x and z .

Despite their smaller number and lower order compared to the number and order of eqns (14), the two Navier equations of plane strain elasticity are in principle more difficult to solve for any set of edge boundary conditions. This is precisely the reason that makes one-dimensional beam theories very useful in practical applications and, therefore, popular among applied scientists and engineers. In what follows, a new method is outlined which is suitable for producing very accurate solutions for any set of edge boundary conditions. The method is based on the formulation of G4DOFBT and may produce accurate solutions provided that the set of the boundary conditions chosen is treated in the averaged sense described by eqns (12).

Assume next that the applied external loading has the following sinusoidal form :

$$q(x) = q_m \sin(\alpha x), \quad \alpha = m\pi/L, \quad (m = 1, 2, \dots). \tag{16}$$

This would be understood as being a simple harmonic in a Fourier sine-series expansion of any relevant loading distribution. Consider finally the particular case in which the beam is subjected to the following type of simply supported edge boundary conditions :

$$\text{at } x = 0, L: \quad N_x^c = w = M_x^c = M_x^a = w_1 = 0. \quad (17)$$

This is the one-dimensional analogue of the following ‘‘point by point’’ set of plane strain, simply supported boundary conditions:

$$\text{at } x = 0, L: \quad \sigma_x = W = 0, \quad (18)$$

employed by Pagano (1969) for the derivation of a corresponding exact elasticity solution.

As may easily be verified, the simply support boundary conditions (17) are satisfied exactly by the following trigonometric displacement representation:

$$\begin{aligned} (u, u_1) &= (A, B) \cos(\alpha x), \\ (w, w_1) &= (C, D) \sin(\alpha x). \end{aligned} \quad (19)$$

Moreover, for the sinusoidally distributed lateral pressure (16), the displacement representation (19) satisfies the Navier-type eqns (14) of G4DOFBT, by converting them into a system of four simultaneous linear algebraic equations for the four unknown constants: A , B , C and D . Hence, for any given set of shape functions, $\varphi(z)$ and $\psi(z)$, the solution of this system of algebraic equations yields a corresponding set of values for all unknown constants, A , B , C and D .

Further details of this procedure for a simply supported beam are given in Section 5 [see eqn (29) below]. It should be mentioned, however, that the simply supported solution is very similar to corresponding solutions available in most textbooks, either for the classical beam theory or for the Timoshenko theory (see, for instance, Donnell, 1976). It should also be emphasised that, for conventional choices of the shape functions $\varphi(z)$ and $\psi(z)$ (Timoshenko, 1922; Bickford, 1982), such a solution will provide reasonably accurate predictions of through-thickness averaged displacements. Nevertheless, it is expected to fail in accurately predicting detailed through-thickness distributions of displacements and stresses, particularly for either thick or highly reinforced beams. It therefore becomes clear that new shape functions should be sought in order to improve the stress analysis performance of G4DOFBT. In the next section, specification of both shape functions is achieved by solving the appropriate plane strain equations of equilibrium of three-dimensional elasticity for the stress distributions caused by the displacement model (1)–(3). This will eventually yield the new method proposed in this paper for improving the stress analysis performance.

4. DETERMINATION OF AN APPROPRIATE SET OF SHAPE FUNCTIONS

The strain field (5) and (6) was obtained by applying the kinematic relations of three-dimensional elasticity to the displacement model (1)–(3) of G4DOFBT. Their introduction into Hooke’s law (13) yields a corresponding three-dimensional stress field, which can therefore be expressed in terms of the four unknown displacement functions u , w , u_1 , w_1 and their spatial derivatives. It may be easily verified that, upon employing the trigonometric displacement representation (19) in connection with that three-dimensional stress field, (i) the plane strain simple support edge boundary conditions (18) are satisfied exactly, and (ii) the two remaining equilibrium equations of plane strain elasticity yield the following set of ordinary differential equations:

$$\begin{aligned} C_{55}^{(r)} B \varphi'' - \alpha^2 C_{11}^{(r)} B \varphi + \alpha (C_{13}^{(r)} + C_{53}^{(r)}) D \psi' &= \alpha^2 C_{11}^{(r)} (A - \alpha z C), \\ C_{33}^{(r)} D \psi'' - \alpha^2 C_{55}^{(r)} D \psi - \alpha (C_{13}^{(r)} + C_{53}^{(r)}) B \varphi' &= -\alpha^2 C_{13}^{(r)} C, \end{aligned} \quad (20)$$

where a prime denotes differentiation with respect to the transverse co-ordinate parameter z .

It is of particular importance to note that the right-hand sides of eqns (20) are entirely dependent upon the basic displacement field (2) while their left-hand-sides depend on the additional corresponding field (3). In this respect, upon ignoring the basic displacement field (or, equivalently, upon setting $A = B = 0$), eqns (20) become equivalent to the fourth-order system of ordinary differential equations employed in the corresponding exact, plane strain elasticity solution obtained by Pagano (1969). This is not a surprising result as, upon setting $A = B = 0$, eqns (1)–(3) and (19) become essentially equivalent to the displacement field employed in Pagano (1969), with the quantities $B\phi(z)$ and $D\psi(z)$ representing the through-thickness unknown distributions of the corresponding displacement components U and W , respectively. Hence, the general solution of eqns (20) can be written in the following form :

$$\begin{pmatrix} B\phi^{(r)}(z) \\ D\psi^{(r)}(z) \end{pmatrix} = \begin{pmatrix} \Phi^{(r)}(z) \\ \Psi^{(r)}(z) \end{pmatrix} + \begin{pmatrix} \alpha \\ 0 \end{pmatrix} Cz - \begin{pmatrix} A \\ C \end{pmatrix}. \tag{21}$$

Here, the layer superscript $^{(r)}$ has been introduced in order to emphasise the dependency of the shape functions on the different elastic properties in each layer. It further emphasises the fact that A , B , C and D are global constants and as such are only dependent upon through-thickness averaged characteristics of the laminated beam considered.

The term that involves the functions Φ and Ψ in the right-hand-side of eqn (21) represents the complementary solution of eqns (20) and, therefore, it coincides with the through-thickness distribution of the exact elasticity solution presented by Pagano (1969). The solution of Pagano’s plane strain problem, in the r th layer of a simply supported cross-ply laminated plate ($r = 1, 2, \dots, N$), can be given in the following form :

$$\begin{aligned} \Phi^{(r)}(z) &= (C_{13}^{(r)} + C_{55}^{(r)}) \sum_{i=1}^4 k_i^{(r)} \lambda_i^{(r)} e^{\alpha \lambda_i^{(r)} z}, \\ \Psi^{(r)}(z) &= \sum_{i=1}^4 k_i^{(r)} (C_{11}^{(r)} - \lambda_i^{(r)2} C_{55}^{(r)}) e^{\alpha \lambda_i^{(r)} z}, \end{aligned} \tag{22}$$

where $\lambda_i^{(r)}$ are the four roots of the following equation :

$$C_{33}^{(r)} C_{55}^{(r)} \lambda^4 - [C_{11}^{(r)} C_{33}^{(r)} - (C_{13}^{(r)})^2 - 2C_{13}^{(r)} C_{55}^{(r)}] \lambda^2 + C_{11}^{(r)} C_{55}^{(r)} = 0, \tag{23}$$

and $k_i^{(r)}$ ($r = 1, 2, \dots, N$; $i = 1, 2, 3, 4$) are $4N$ unknown constants.

It is worth-mentioning that the Φ - and Ψ -functions are exponential functions of the transverse co-ordinate, z , with the exponents being dependent on the material and the geometrical properties of the beam considered. The $4N$ unknown constants could be determined, by using a standard numerical routine, from an equal number of interface continuity and lateral plane boundary conditions briefly outlined next. Accordingly, the continuity of displacements at all material interfaces $z = h_r$ ($r = 2, 3, \dots, N$) of a simply supported plate implies,

$$\Phi^{r-1}(h_r) - \Phi^{(r)}(h_r) = 0, \quad \Psi^{(r-1)}(h_r) - \Psi^{(r)}(h_r) = 0. \tag{24a}$$

Moreover, continuity of the interlaminar stresses, σ_z and τ_{xz} , at those material interfaces of a simply supported plate implies,

$$\begin{aligned} -\alpha C_{13}^{(r-1)} \Phi^{(r-1)}(h_r) + C_{33}^{(r-1)} \Psi^{(r-1)'}(h_r) + \alpha C_{13}^{(r)} \Phi^{(r)}(h_r) - C_{33}^{(r)} \Psi^{(r)'}(h_r) &= 0, \\ C_{55}^{(r-1)} (\Phi^{(r-1)'}(h_r) + \alpha \Psi^{(r-1)}(h_r)) - C_{55}^{(r)} (\Phi^{(r)'}(h_r) + \alpha \Psi^{(r)}(h_r)) &= 0, \end{aligned} \tag{24b}$$

$(r = 2, 3, \dots, N).$

Finally, the stress lateral surface boundary conditions are,

$$\begin{aligned}
 -\alpha C_{13}^{(1)}\Phi^{(1)}(h_1) + C_{33}^{(1)}\Psi^{(1)'}(h_1) &= 0, \\
 \Phi^{(1)'}(h_1) + \alpha\Psi^{(1)}(h_1) &= 0, \\
 -\alpha C_{13}^{(N)}\Phi^{(N)}(h_{N+1}) + C_{33}^{(N)}\Psi^{(N)'}(h_{N+1}) &= -q_m, \\
 \Phi^{(N)'}(h_{N+1}) + \alpha\Psi^{(N)}(h_{N+1}) &= 0,
 \end{aligned} \tag{24c}$$

where h_1 and h_{N+1} represent the value of the transverse co-ordinate at the bottom and the top lateral planes of the plate, respectively.

The last two terms of eqn (21) represent a particular integral of eqns (20). As they both cancel by setting $A = C = 0$, they may be thought of as eliminating the inaccuracies that have been superposed onto the corresponding exact elasticity solution (Φ and Ψ) by the basic displacement field (2) of G4DOFBT. This is verified by the fact that the two shape functions defined in eqn (21) satisfy the equations of three-dimensional elasticity independently of the values of the unknown constants A , B , C and D . Moreover, by means of eqns (1)–(3), (19) and (21), they always yield the exact elasticity solution presented by Pagano (1969) for cylindrical bending of simply supported infinite strips.

These arguments show that, as far as flexure of simply supported beams is concerned, values can be assigned to those unknown constants in an almost arbitrary manner. In doing so, the only requirement is that non-zero values should be assigned to B and D , as nullification of one or both of these constants is equivalent to neglecting, partially or entirely, the effects of transverse deformation. It therefore becomes evident that eqn (21) represents a four-parameter family of shape functions, each set of which serves equally well the purposes of the analysis presented; provided that non-zero values are assigned to B and D , any set of shape functions $\varphi(z)$ and $\psi(z)$, produced by means of eqns (21), satisfies exactly the equations of three-dimensional elasticity for that particular flexure problem of simply supported beams. This further reflects the fact that the equations of equilibrium (11) of G4DOFBT are of no use in dealing with flexure of simply supported plates. With any set of such shape functions, equations of equilibrium (11) may yield corresponding “improved” values to all A , B , C and D which, however, still yield, through eqns (1)–(3), (19) and (21), the exact, plane strain elasticity solution (Pagano, 1969).

Nevertheless, the above results lead to an important conclusion, namely that, as far as accurate stress analysis is concerned, the above procedure is capable of opening up new directions to the restricted usefulness of one-dimensional beam and two-dimensional plate and shell theories. Accordingly, the equations of equilibrium (11) of G4DOFBT can be used, in conjunction with the shape functions (21), for the accurate stress analysis of corresponding elastic beams, the edges of which are subjected to boundary conditions that differ from the simply supported boundary conditions (18). In such cases, however, eqn (21) may no longer be considered as representing an infinite number of equivalent sets of shape functions, but certain particular values should be assigned to all A , B , C and D in a manner that appropriately serves the fundamental ideas upon which G4DOFBT is built. An obvious way to do so is to introduce eqn (21) to the four constraint eqns (4). This yields four algebraic equations, the solution of which provides the following unique values to all of A , B , C and D :

$$\begin{aligned}
 A &= (C_{13}^{(ca)} + C_{55}^{(ca)}) \sum_{i=1}^4 k_i^{(ca)} \lambda_i^{(ca)}, \\
 B &= \alpha \sum_{i=1}^4 k_i^{(ca)} [C_{11}^{(ca)} + (\lambda_i^{(ca)})^2 C_{13}^{(ca)}], \\
 C &= \sum_{i=1}^4 k_i^{(ca)} [C_{11}^{(ca)} - (\lambda_i^{(ca)})^2 C_{55}^{(ca)}],
 \end{aligned}$$

$$D = \alpha \sum_{i=1}^4 k_i^{(ca)} \lambda_i^{(ca)} [C_{11}^{(ca)} - (\lambda_i^{(ca)})^2 C_{55}^{(ca)}]. \tag{25}$$

Here, quantities indicated by a superscript ^(ca) are related to the layer that contains the central axis of the beam considered.

In order to show the effectiveness of the method proposed in this paper, two examples are considered in the next section. Both examples deal with displacement and stress distributions within a homogeneous or a laminated beam having one edge rigidly clamped and the other edge either free or guided.

5. FLEXURE OF BEAMS WITH REALISTIC EDGE BOUNDARY CONDITIONS

The general solution of the system of ordinary differential eqns (14) can be written in the following form, which is independent of the choice of the shape functions :

$$\begin{aligned} u &= \frac{1}{F_1} \left\{ \sum_{i=1}^4 \frac{1}{\mu_i} [A_{55}^{aa} F_1 F_5 + \mu_i^2 (F_3 G_2 - F_5 G_1)] K_i e^{\mu_i x} + Q_3 K_5 x - Q_2 (\frac{1}{2} K_6 x^2 + K_7 x) + K_8 \right\} \\ &\quad + \tilde{A} \cos \alpha x, \\ w &= \frac{1}{F_1} \left\{ \sum_{i=1}^4 \frac{1}{\mu_i^2} [A_{55}^{aa} F_1 F_4 + \mu_i^2 (F_2 G_2 - F_4 G_1)] K_i e^{\mu_i x} + \frac{1}{2} Q_2 K_5 x^2 \right. \\ &\quad \left. - Q_1 (\frac{1}{6} K_6 x^3 + \frac{1}{2} K_7 x^2) + K_9 x + K_{10} \right\} \\ &\quad + \tilde{C} \sin \alpha x, \\ u_1 &= \sum_{i=1}^4 \mu_i G_2 K_i e^{\mu_i x} + \frac{F_2 G_4 - F_4 G_2}{A_{55}^{aa} F_1 G_4} K_6 + \tilde{B} \cos \alpha x, \\ w_1 &= \sum_{i=1}^4 (A_{55}^{aa} F_1 - \mu_i^2 G_1) K_i e^{\mu_i x} + \frac{F_5}{G_4} K_5 - \frac{F_4}{G_4} (K_6 x + K_7) + \tilde{D} \sin \alpha x. \end{aligned} \tag{26}$$

Here,

$$\begin{aligned} F_1 &= A_{11}^c D_{11}^c - B_{11}^{c^2}, \quad F_2 = A_{11}^c D_{11}^a - B_{11}^c B_{11}^a, \quad F_3 = B_{11}^c D_{11}^a - D_{11}^c B_{11}^a, \\ F_4 &= A_{11}^c D_{13}^b - B_{11}^c B_{13}^b, \quad F_5 = B_{11}^c D_{13}^b - D_{11}^c B_{13}^b, \\ G_1 &= B_{11}^a F_3 - D_{11}^a F_2 + D_{11}^{aa} F_1, \quad G_2 = B_{11}^a F_5 - D_{11}^a F_4 + (D_{13}^{ab} - A_{55}^{ab}) F_1, \\ G_3 &= B_{13}^b F_3 - D_{13}^b F_2 + (D_{13}^{ab} - A_{55}^{ab}) F_1, \quad G_4 = B_{13}^b F_5 - D_{13}^b F_4 + D_{33}^{bb} F_1, \\ Q_1 &= A_{11}^c + \frac{F_4^2}{G_4}, \quad Q_2 = B_{11}^c + \frac{F_4 F_5}{G_4}, \quad Q_3 = D_{11}^c + \frac{F_5^2}{G_4}, \end{aligned} \tag{27}$$

while μ_i are the four roots of the following equation :

$$A_{55}^{bb} F_1 G_1 \mu^4 - (G_1 G_4 - G_2 G_3 + A_{55}^{bb} A_{55}^{aa} F_1^2) \mu^2 + A_{55}^{aa} F_1 G_4 = 0. \tag{28}$$

The trigonometric terms that appear in eqns (26) represent the particular integral of eqns (14) and clearly have the form (19) for the corresponding solution of the flexure problem of a simply supported beam. Their constant coefficients are determined from the solution of the following set of linear algebraic equations :

$$\begin{bmatrix} -\alpha^2 A_{11}^c & \alpha^3 B_{11}^c & -\alpha^2 B_{11}^a & \alpha B_{11}^b \\ \alpha^3 B_{11}^c & -\alpha^4 D_{11}^c & \alpha^3 D_{11}^a & -\alpha^2 D_{13}^b \\ -\alpha^2 B_{11}^a & \alpha^3 D_{11}^a & -\alpha^2 D_{11}^{aa} - A_{55}^{aa} & \alpha(D_{13}^{ab} - A_{55}^{ab}) \\ \alpha B_{11}^a & -\alpha^2 D_{13}^b & \alpha(D_{13}^{ab} - A_{55}^{ab}) & -\alpha^2 A_{55}^{bb} - D_{33}^{bb} \end{bmatrix} \begin{bmatrix} \tilde{A} \\ \tilde{C} \\ \tilde{B} \\ \tilde{D} \end{bmatrix} = \begin{bmatrix} 0 \\ q_m \\ 0 \\ \psi(h/2)q_m \end{bmatrix}. \quad (29)$$

As eqns (15) make clear, the values of \tilde{A} , \tilde{B} , \tilde{C} and \tilde{D} are dependent on the choice of the shape functions. For the reasons detailed in the preceding section, however, the shape functions (21) to be used in these examples are extracted from Pagano's (1969) elasticity solution for simply supported plates. It can be verified numerically that, after this choice of shape functions, the coefficients \tilde{A} , \tilde{B} , \tilde{C} and \tilde{D} determined through eqns (29) have identical values to the corresponding constants A , B , C and D determined through eqns (25). Although this is not at all obvious, it simply confirms that this method yields the exact elasticity solution when both plate edges are simply supported. As briefly outlined below, this is also in complete mathematical agreement with the fact that, for simply supported plates, all ten constants K_i ($i = 1, 2, \dots, 10$) appearing in eqns (26) take zero values.

The ten arbitrary constants of integration K_i ($i = 1, 2, \dots, 10$) are free to be determined by means of an appropriate set of boundary conditions imposed at the edges $x = 0$ and $x = L$ of the beam. Connecting eqns (26) with the chosen set of edge boundary conditions always yields a 10×10 system of linear algebraic equations, which may be represented in the following matrix form:

$$\mathbf{MK} = \mathbf{B}. \quad (30)$$

For the clamped-free and clamped-guided supported beams considered in this paper, the elements of the matrix \mathbf{M} , as well as the elements of the column vector \mathbf{B} , are given in the Appendix. It should be noted that independent of the set of edge boundary conditions the elements of \mathbf{B} and, therefore, the values of K_i ($i = 1, 2, \dots, 10$) are always dependent on \tilde{A} , \tilde{C} , \tilde{B} and \tilde{D} . In the particular case, however, of a beam having both of its edges simply supported, the edge values of the trigonometric functions involved in eqns (26) yield zero values to all elements of \mathbf{B} . Hence, eqn (30) yields $K_i = 0$ ($i = 1, 2, \dots, 10$) and eqns (26) are naturally reduced to their appropriate trigonometric form (19).

For beams not having both of their edges simply supported, the satisfaction of eqns (24a) still guarantees the interlaminar continuity of the displacement components, despite the appearance of the non-zero constants K_i ($i = 1, 2, \dots, 10$). The form, however, of the corresponding transverse shear and normal stress components becomes very complicated. Hence, the satisfaction of eqns (24b) and (24c) no longer guarantees the prediction of continuous interlaminar stresses or the exact satisfaction of the stress boundary conditions imposed on the lateral planes of the plate. A way to try and avoid this source of inaccuracy is by leaving eqns (24b) and (24c) unsatisfied and, hence, by requiring that all K_i ($i = 1, 2, \dots, 10$) should become functions of the $4N$ constants $k_i^{(r)}$ ($r = 1, 2, \dots, N$; $i = 1, 2, 3, 4$), through eqns (15) and (27). Then one may be able to replace eqns (24b) and (24c) with a corresponding set of $2N + 2$ algebraic equations which will give a more accurate representation of both the continuity of the interlaminar stresses and the satisfaction of the stress boundary conditions imposed on the lateral planes. These, together with eqns (24a), will eventually yield a highly non-linear system of $4N$ algebraic equations, for the same number of unknown constants $k_i^{(r)}$ ($r = 1, 2, \dots, N$; $i = 1, 2, 3, 4$).

Such a laborious and numerically complicated procedure will not be employed in the present study, as its success is currently uncertain while a possible improvement of the results obtained might be found to be practically unimportant. Instead, to keep the analysis simple, the stress continuity conditions and the lateral surface boundary conditions will only be satisfied in the simple support sense, which has already been outlined and is closely connected to Pagano's (1969) plane strain elasticity solution. As will become obvious in

the next section, such a strategy is still able to produce very accurate displacement and stress distributions, as it is in keeping with the concept that away from the edges of the body ($x = 0, L$) the solution is that for simply supported edges.

6. NUMERICAL RESULTS AND DISCUSSION

As has already been mentioned, all results that are presented and discussed in this paper are for beams that have one edge rigidly clamped and the other either free or guided. Under these considerations, the following boundary conditions are imposed at $x = 0$:

$$u_0 = w_0 = w_{0,x} = u_1 = w_1 = 0, \quad (31)$$

which is, therefore, assumed as always being the rigidly clamped edge of the plate. For a clamped-free beam, the following boundary conditions are assumed at $x = L$:

$$N_x^c = M_{x,x}^c = M_x^c = M_x^a = P_x^a = 0. \quad (32)$$

Finally, for a clamped-guided beam, the following boundary conditions are assumed at $x = L$:

$$u_0 = M_{x,x}^c = w_{0,x} = u_1 = P_x^a = 0. \quad (33)$$

For either case, the elements of the matrix \mathbf{M} and the column vector \mathbf{B} that appear in eqn (30) are given in the Appendix. Finally, note that the sets of edge boundary conditions described by eqns (31)–(33) are the one-dimensional analogues of the following “point by point” sets of plane strain conditions:

$$\begin{aligned} \text{at a clamped edge: } & U = W = 0, \\ \text{at a free edge: } & \sigma_x = \tau_{xz} = 0, \\ \text{at a guided edge: } & U = \tau_{xz} = 0. \end{aligned} \quad (34)$$

The orthotropic material in all of the applications considered has the following elastic properties:

$$E_L/E_T = 40, \quad G_{LT}/E_T = 0.5, \quad G_{TT}/E_T = 0.2, \quad \nu_{LT} = \nu_{TT} = 0.25, \quad (35)$$

where the subscripts L and T denote properties associated with the longitudinal and the transverse fibre direction, respectively. Two different plate lay-ups are considered: (i) homogeneous plates with fibres aligned to the x -axis; and (ii) two-layered antisymmetric cross-ply, with the material interface placed at $z/h = 0.2$ and with fibres aligned to the x -axis in the bottom layer. In the case of a regular antisymmetric lay-up, in which both layers have equal thickness, the plate middle-plane coincides with the material interface and, as a result, the last of eqns (4a) and (24b) force the transverse shear stress to be continuous across the material interface. Hence, the particular lay-up employed in case (ii) has been selected in an attempt to magnify the effects of the aforementioned possible discontinuity of the interlaminar stresses and, therefore, to quantitatively estimate the extent to which it can affect the accuracy of the results obtained. The beam thickness considered in all cases is determined by the ratio $h/L = 0.25$. This characterises a very thick beam and, in conjunction with the high value of the stiffness ratio E_L/E_T , is considered to be an adequate test for the validity and the reliability of the new method. The integer value that characterises the particular harmonic employed in the Fourier sine-series expansion of any loading distribution applied on the top lateral plane of the plate is taken as $m = 1$ [see eqn (16)].

Table 1. Displacement distributions for a clamped-free homogeneous beam

	z/h	x/L					
		0.0	0.2	0.4	0.6	0.8	1.0
$E_T U_j / L q_1$	0.5	0.0000	0.2216	0.2663	0.2624	0.2434	0.2338
	0.4	0.0000	0.1020	0.1567	0.1797	0.1856	0.1861
	0.3	0.0000	0.0443	0.0936	0.1222	0.1358	0.1397
	0.2	0.0000	0.0172	0.0534	0.0770	0.0898	0.0938
	0.1	0.0000	0.0045	0.0241	0.0377	0.0456	0.0482
	0.0	0.0000	-0.0022	-0.0008	0.0009	0.0022	0.0028
	-0.1	0.0000	-0.0086	-0.0255	-0.0359	-0.0411	-0.0427
	-0.2	0.0000	-0.0200	-0.0539	-0.0747	-0.0851	-0.0882
	-0.3	0.0000	-0.0443	-0.0921	-0.1187	-0.1307	-0.1340
	-0.4	0.0000	-0.0962	-0.1508	-0.1739	-0.1799	-0.1804
	-0.5	0.0000	-0.2041	-0.2516	-0.2519	-0.2361	-0.2278
$E_T W_j / L q_1$	0.5	0.0000	-1.0032	-2.2204	-3.1559	-3.7501	-4.1320
	0.4	0.0000	-0.9879	-2.1990	-3.1351	-3.7373	-4.1292
	0.3	0.0000	-0.9730	-2.1780	-3.1147	-3.7248	-4.1266
	0.2	0.0000	-0.9594	-2.1590	-3.0962	-3.7134	-4.1242
	0.1	0.0000	-0.9478	-2.1426	-3.0802	-3.7036	-4.1221
	0.0	0.0000	-0.9382	-2.1292	-3.0672	-3.6956	-4.1204
	-0.1	0.0000	-0.9308	-2.1188	-3.0571	-3.6894	-4.1191
	-0.2	0.0000	-0.9255	-2.1114	-3.0498	-3.6849	-4.1181
	-0.3	0.0000	-0.9220	-2.1064	-3.0450	-3.6820	-4.1175
	-0.4	0.0000	-0.9198	-2.1034	-3.0420	-3.6802	-4.1171
	-0.5	0.0000	-0.9180	-2.1009	-3.0396	-3.6787	-4.1168

At selected points within a homogeneous clamped-free orthotropic beam, Tables 1 and 2 present numerical values of normalised displacement and stress distributions, respectively. Corresponding complete in-plane displacement, bending stress and shear stress distributions are shown graphically in Figs 1, 2 and 3, respectively. Although the plots in these figures appear to have a certain symmetry with respect to the central axis of the beam ($z = 0$), a closer inspection of the results tabulated in Tables 1 and 2 will reveal that this is not so. Contrary to what happens in corresponding two- and one-dimensional theories that ignore the effects of transverse normal deformation ($w_1 = 0$), here the transverse displacement component, W , varies through the beam thickness in a non-uniform manner. With the external loading being applied to the upper lateral plane, this variation is more pronounced in the upper rather than in the bottom half of the beam. Hence, although the variation of W is not large enough to substantially influence the much higher values of the bending and the transverse shear stress distributions, it makes the corresponding absolute values of these distributions slightly higher in the upper as opposed to the bottom half of the beam. It is observed that the present approach enables the prediction of the well-known boundary layer behaviour of the bending stress, σ_x , near the lateral planes of the beam, thus eliminating the main stress-analysis drawback of all conventional one-dimensional beam theories.

An interesting feature of the results shown in Table 2 deals with the extent to which the stress boundary conditions imposed on the lateral planes of the beam are satisfied. Table 2 reveals that, as far as the transverse shear stress τ_{xz} is concerned and away from a narrow zone at the clamped edge, the absolute value of the relative error is less than 5% at the bottom lateral plane ($z = -h/2$). At the top layer, the absolute value of the relative error of τ_{xz} is higher, but this, measured with respect to the maximum values of τ_{xz} on a beam cross-section, is still very small. This is illustrated more clearly in Fig. 3 and means that, away from the clamped edge, the present method is practically satisfying the zero shear traction boundary condition imposed on the bottom lateral plane while it fails only slightly to satisfy the corresponding boundary condition on the top lateral plane of the beam. The trend of the results plotted in Fig. 3 shows that the amplitude of the nearly parabolic shear stress distribution is initially increasing with increasing distance from the free edge of the beam ($x/L = 1.0$). Upon approaching the clamped edge, however, results that are not shown here reveal that the amplitude of the τ_{xz} -distribution is gradually

Table 2. Stress distributions for a clamped-free homogeneous beam

		x/L					
		0.0	0.2	0.4	0.6	0.8	1.0
σ_x/q_1	z/h						
	0.5	111.9400	16.8157	2.5881	-3.5757	-3.6636	-0.0004
	0.4	27.2994	14.9149	7.0377	2.1467	0.1721	-0.0002
	0.3	-6.1687	11.8125	7.4049	3.7537	1.4576	0.0000
	0.2	-14.4531	8.1186	5.7626	3.3352	1.4878	0.0001
	0.1	-10.7473	4.1428	3.1634	1.9519	0.9201	0.0002
	0.0	-2.1481	0.0518	0.1732	0.1746	0.1082	0.0002
	-0.1	6.7405	-4.0464	-2.8404	-1.6264	-0.7184	0.0002
	-0.2	11.4678	-8.0471	-5.5225	-3.0932	-1.3378	0.0001
	-0.3	5.4760	-11.7965	-7.3499	-3.6983	-1.4233	0.0000
	-0.4	-23.2307	-15.0129	-7.3657	-2.4772	-0.3770	-0.0002
-0.5	-98.1770	-17.1442	-3.6936	2.4616	2.9733	-0.0006	
σ_y/q_1	0.5	0.9328	-0.0180	-0.2002	-0.2457	-0.1630	-0.0282
	0.4	0.2275	-0.0394	-0.1710	-0.2057	-0.1357	-0.0292
	0.3	-0.0514	-0.0548	-0.1533	-0.1780	-0.1163	-0.0273
	0.2	-0.1204	-0.0674	-0.1415	-0.1567	-0.1008	-0.0241
	0.1	-0.0896	-0.0789	-0.1327	-0.1386	-0.0874	-0.0202
	0.0	-0.0179	-0.0901	-0.1255	-0.1221	-0.0749	-0.0161
	-0.1	0.0562	-0.1015	-0.1187	-0.1061	-0.0627	-0.0121
	-0.2	0.0956	-0.1136	-0.1113	-0.0893	-0.0501	-0.0083
	-0.3	0.0456	-0.1272	-0.1018	-0.0703	-0.0361	-0.0052
	-0.4	-0.1936	-0.1439	-0.0877	-0.0463	-0.0189	-0.0033
	-0.5	-0.8181	-0.1665	-0.0639	-0.0117	0.0050	-0.0042
σ_z/q_1	0.5	0.9328	-0.4922	-0.8654	-0.8933	-0.5604	-0.1127
	0.4	0.2275	-0.5306	-0.8600	-0.8764	-0.5473	-0.1167
	0.3	-0.0514	-0.5147	-0.7982	-0.8059	-0.5015	-0.1093
	0.2	-0.1204	-0.4727	-0.7099	-0.7101	-0.4404	-0.0963
	0.1	-0.0896	-0.4192	-0.6100	-0.6033	-0.3725	-0.0809
	0.0	-0.0179	-0.3616	-0.5063	-0.4929	-0.3024	-0.0645
	-0.1	0.0562	-0.3047	-0.4038	-0.3836	-0.2330	-0.0483
	-0.2	0.0956	-0.2532	-0.3071	-0.2799	-0.1671	-0.0332
	-0.3	0.0456	-0.2140	-0.2235	-0.1888	-0.1088	-0.0206
	-0.4	-0.1936	-0.2001	-0.1666	-0.1231	-0.0660	-0.0134
	-0.5	-0.8181	-0.2373	-0.1633	-0.1085	-0.0544	-0.0168
τ_{xz}/q_1	0.5	-0.7812	0.1709	0.1511	0.1500	0.1483	0.0246
	0.4	-0.5978	-1.5353	-1.1335	-0.5616	-0.0984	-0.0131
	0.3	-0.4182	-2.3705	-1.7650	-0.9193	-0.2338	-0.0340
	0.2	-0.2552	-2.7695	-2.0689	-1.0981	-0.3110	-0.0461
	0.1	-0.1150	-2.9440	-2.2039	-1.1834	-0.3559	-0.0532
	0.0	0.0000	-2.9903	-2.2420	-1.2141	-0.3804	-0.0573
	-0.1	0.0891	-2.9381	-2.2054	-1.2021	-0.3882	-0.0587
	-0.2	0.1533	-2.7653	-2.0778	-1.1385	-0.3766	-0.0572
	-0.3	0.1953	-2.3874	-1.7957	-0.9894	-0.3354	-0.0511
	-0.4	0.2212	-1.6141	-1.2167	-0.6782	-0.2412	-0.0370
	-0.5	0.2431	-0.0532	-0.0470	-0.0467	-0.0462	-0.0077

decreasing, while its shape still remains nearly parabolic. Further, it practically satisfies the imposed lateral plane boundary conditions and it is only in a very narrow band, very close to the edge ($x/L < 0.05$), in which the through thickness distribution of τ_{xz} starts to gradually take the shape of the solid line shown in Fig. 3. Under these considerations, the fact that the solid line shown in Fig. 3 does not satisfy the lateral boundary conditions is not necessarily erroneous. This may be considered to be due to the fact that the two corners of the edge (at $x/L = 0$ and $z = \pm h/2$) are singular points for the boundary value problem considered and, therefore, τ_{xz} may indeed take non-zero values at those two points.

Similar observations can be made with regard to the values of the transverse normal stress σ_z predicted at the lateral planes (Table 2). At the bottom plane of the beam, where no loading is applied, the predicted values of σ_z are again small away from the clamped edge. It appears that the relative error is as high as about 5% at $x/L = 0.8$ and is continuously increasing when approaching the clamped edge. With the values of σ_z , however, being in general much smaller than the corresponding values of τ_{xz} , and two orders of

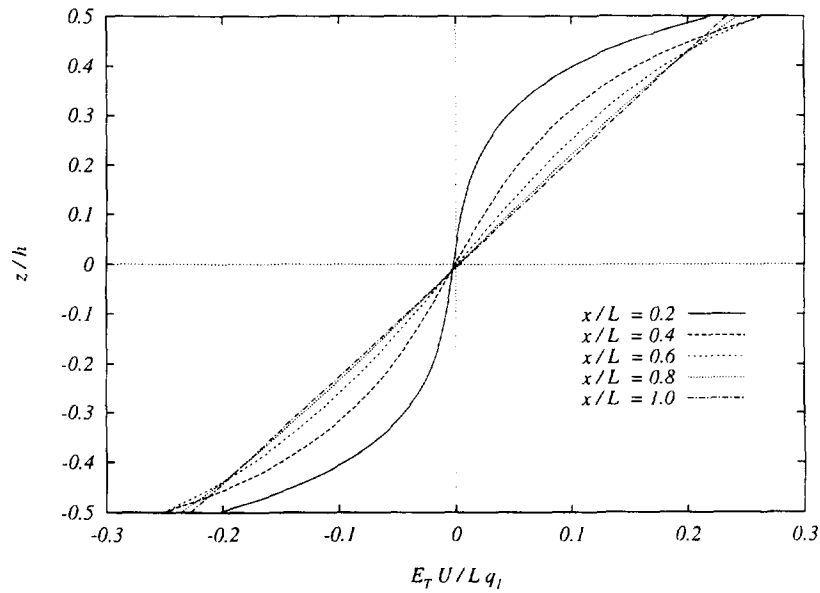


Fig. 1. In-plane displacement distributions for a clamped-free homogeneous beam.

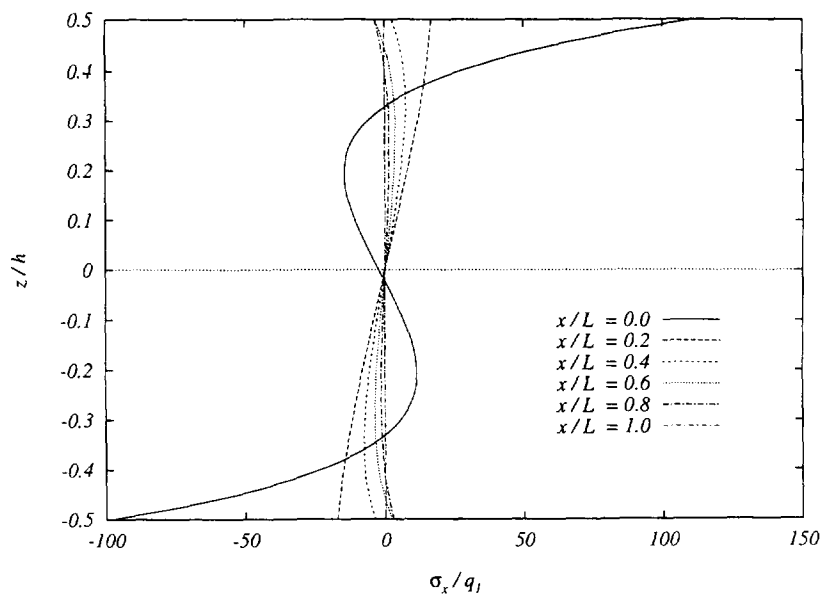


Fig. 2. Bending stress distributions for a clamped-free homogeneous beam.

magnitude smaller than σ_{xy} , such errors are not expected to substantially influence the accuracy of the other numerical results obtained and presented in this paper. Moreover, Fig. 4 shows that there is a very good agreement between the distribution of σ_z predicted on $z = h/2$ and the corresponding, exact, sinusoidal, external stress distribution applied on the top lateral plane of the beam. The only apparent difference is again in a small region around the corner of each edge, particularly the clamped one. Figure 4 also compares the sinusoidal, external stress distribution applied to the top lateral plane of a two-layered clamped-free beam with the corresponding σ_z -distribution predicted on the basis of the present analysis.

At selected points within a two-layered clamped-free beam, Tables 3 and 4 present detailed numerical values of normalised displacement and stress distributions, respectively. Corresponding complete in-plane displacement, bending stress and shear stress distributions are plotted in Figs 5, 6 and 7, respectively. It should be noticed, that two sets of values are quoted at the interface of the laminate (one each for the layer above and below $z/h = 0.2$),

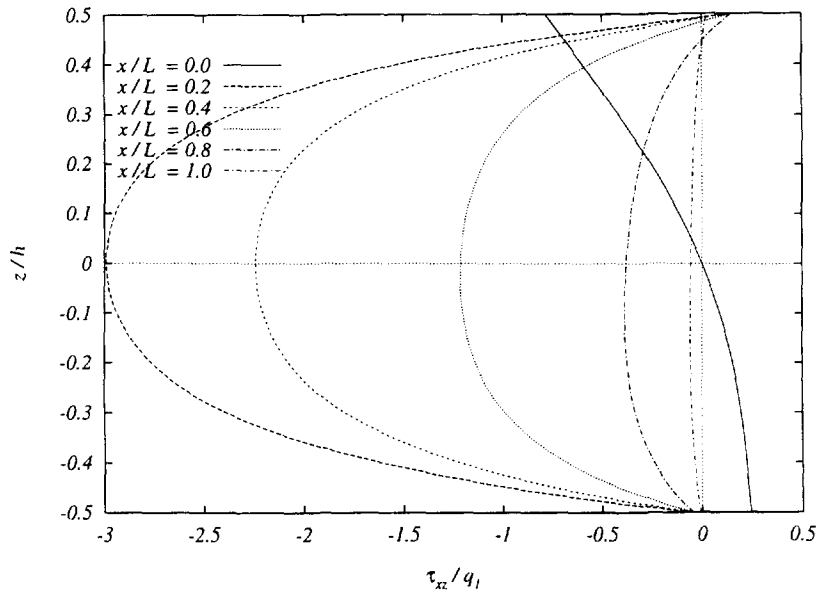


Fig. 3. Shear stress distributions for a clamped-free homogeneous beam.

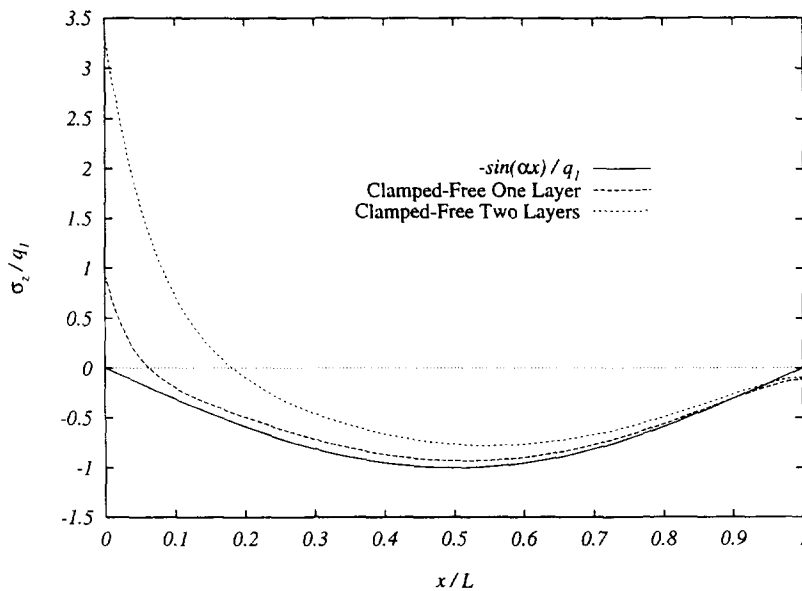


Fig. 4. Fit of transverse normal stress at upper lateral surface for clamped-free beams.

thus illustrating that the present analysis satisfies continuity of displacements (Table 3) but it fails to satisfy exactly continuity of interlaminar stresses (Table 4).

It should be noted, however, that the discontinuity of the interlaminar stresses is very small and is practically negligible away from the clamped edge. This latter observation becomes obvious in Fig. 7 where, away from the edge, the through-thickness distribution of τ_{xz} looks essentially continuous at $z/h = 0.2$. The discontinuity of both τ_{xz} and σ_z becomes, however, more evident at the point where the clamped edge ($x = 0$) intersects with the material interface ($z/h = 0.2$). Although this is again not expected to particularly influence the accuracy of the relevant numerical results away from the edge, it has an additive effect on the aforementioned small error which is due to the singular nature of the corner edge points. As a result, the slight disagreement between the predicted and the applied values of the external stress distribution applied on the top lateral plane has further increased in the case of a two-layered beam (Fig. 4). This, however, cannot be considered as a serious disadvantage of the present method, mainly because the values of σ_z are considerably lower than the values of the other stresses and are, therefore, most sensitive to small errors.

Table 3. Displacement distributions for a clamped-free two-layered beam

	z/h	x/L					
		0.0	0.2	0.4	0.6	0.8	1.0
$E_T U/Lq_1$	0.5	0.0000	0.9276	1.0489	0.9816	0.8708	0.8229
	0.4	0.0000	0.6892	0.8152	0.7914	0.7246	0.6940
	0.3	0.0000	0.4794	0.6030	0.6128	0.5820	0.5657
	0.2	0.0000	0.2920	0.4076	0.4432	0.4421	0.4378
	0.2	0.0000	0.2920	0.4076	0.4432	0.4421	0.4378
	0.1	0.0000	0.1344	0.2347	0.2858	0.3059	0.3105
	0.0	0.0000	0.0561	0.1217	0.1606	0.1795	0.1848
	-0.1	0.0000	0.0133	0.0353	0.0497	0.0574	0.0598
	-0.2	0.0000	-0.0202	-0.0440	-0.0574	-0.0635	-0.0650
	-0.3	0.0000	-0.0654	-0.1321	-0.1692	-0.1858	-0.1901
	-0.4	0.0000	-0.1495	-0.2496	-0.2968	-0.3129	-0.3159
	-0.5	0.0000	-0.3195	-0.4318	-0.4593	-0.4507	-0.4434
	$E_T W/Lq_1$	0.5	0.0000	-1.4715	-3.4674	-5.1902	-6.4974
0.4		0.0000	-1.4589	-3.4503	-5.1744	-6.4879	-7.5314
0.3		0.0000	-1.4442	-3.4303	-5.1559	-6.4769	-7.5284
0.2		0.0000	-1.4279	-3.4081	-5.1353	-6.4645	-7.5250
0.2		0.0000	-1.4279	-3.4081	-5.1353	-6.4645	-7.5250
0.1		0.0000	-1.4112	-3.3853	-5.1142	-6.4518	-7.5215
0.0		0.0000	-1.3954	-3.3639	-5.0943	-6.4399	-7.5183
-0.1		0.0000	-1.3823	-3.3461	-5.0778	-6.4300	-7.5156
-0.2		0.0000	-1.3725	-3.3327	-5.0655	-6.4226	-7.5136
-0.3		0.0000	-1.3660	-3.3238	-5.0572	-6.4177	-7.5122
-0.4		0.0000	-1.3619	-3.3182	-5.0520	-6.4146	-7.5113
-0.5		0.0000	-1.3583	-3.3134	-5.0476	-6.4119	-7.5106

Moreover, with this method being based on what is essentially a one-dimensional laminated beam theory, a remarkable credibility should be recognised for the vast majority if not for all of the numerical results presented and discussed.

This latter argument is substantially reinforced by the fact that the boundary conditions imposed at the edges of either a homogeneous or a two-layered beam have been satisfied in a very satisfactory degree [see also eqns (34a) and (34b)]. Tables 1 and 3 show that, indeed, the clamped edge boundary conditions are satisfied in a three-dimensional, point by point sense, as both the in-plane and the transverse displacement components have taken zero values at the $x = 0$, for all values of z . Moreover, the distributions of σ_x and τ_{xz} are very small and, practically, negligible at the free edge ($x/L = 1$) of either a homogeneous or a two-layered beam. The corresponding numerical results tabulated in Tables 5, 6 and 7, 8 for homogeneous orthotropic and two-layered beams, respectively, are also in favour of this argument.

The numerical results tabulated in Tables 5–8 as well as the ones plotted in Figs 8–14 correspond to the results shown in Tables 1–4 and Figs 1–7, respectively, but they are for beams having their left edge clamped and the other guided. The validity of the above argument, which further substantiates the validity of the present approach, is again confirmed as, either in the clamped or in the guided edge, the boundary conditions are now satisfied exactly, in a three-dimensional, point by point sense [see also eqns (34a) and (34c)]. As was expected, due to the left clamped edge, the shapes of the displacement and stress distributions in the left part of a clamped-guided beam are very similar to those already presented and discussed for a corresponding clamped-free beam. The right guided edge, however, has absorbed a part of the high flexibility of the cantilevered beam. This has decreased the reactions around the clamped edge, and can be verified by comparing corresponding displacement values tabulated in Tables 1 and 5 or in Tables 3 and 7. As a result, the values of all stresses in a clamped-guided beam are slightly higher in the left part of the beam, and are considerably higher in its right part, compared to their values in a corresponding clamped-free beam.

Table 4. Stress distributions for a clamped-free two-layered beam

		x/L							
		z/h	0.0	0.2	0.4	0.6	0.8	1.0	
σ_x/q_1	0.5		13.1744	1.4377	-0.1727	-0.7441	-0.5903	0.0011	
	0.4		9.1656	1.2115	-0.0364	-0.5127	-0.4264	-0.0122	
	0.3		5.7529	0.9783	0.0559	-0.3266	-0.2905	-0.0231	
	0.2		2.8025	0.7397	0.1140	-0.1755	-0.1763	-0.0323	
	0.2		105.2589	34.4588	13.3677	1.8287	-1.5725	0.1703	
	0.1		17.7546	25.6104	14.3576	6.2290	1.9208	-0.0010	
	0.0		-7.8258	15.5230	10.0772	5.2922	2.1272	-0.0355	
	-0.1		-5.7845	4.8827	3.4456	1.9744	0.8672	-0.0090	
	-0.2		3.6075	-5.9050	-3.8121	-1.9774	-0.7833	0.0336	
	-0.3		3.8171	-16.5094	-10.2889	-5.1383	-1.9467	0.0558	
	-0.4		-26.3449	-26.5067	-14.1814	-5.6822	-1.4983	0.0109	
	-0.5		-123.4826	-35.1648	-12.3749	-0.4546	2.5046	-0.1822	
	σ_y/q_1	0.5		4.1235	0.3362	-0.2088	-0.3763	-0.2708	-0.0232
		0.4		2.8687	0.2420	-0.1981	-0.3335	-0.2372	-0.0322
0.3			1.8006	0.1504	-0.1944	-0.2986	-0.2087	-0.0395	
0.2			0.8772	0.0609	-0.1964	-0.2700	-0.1842	-0.0454	
0.2			0.8772	0.1135	-0.1249	-0.2037	-0.1444	-0.0345	
0.1			0.1480	0.0358	-0.1220	-0.1721	-0.1183	-0.0368	
0.0			-0.0652	-0.0264	-0.1279	-0.1522	-0.1000	-0.0325	
-0.1			-0.0482	-0.0818	-0.1380	-0.1380	-0.0854	-0.0254	
-0.2			0.0301	-0.1357	-0.1495	-0.1256	-0.0719	-0.0176	
-0.3			0.0318	-0.1923	-0.1601	-0.1118	-0.0576	-0.0108	
-0.4			-0.2195	-0.2568	-0.1671	-0.0927	-0.0397	-0.0073	
-0.5			-1.0290	-0.3389	-0.1655	-0.0616	-0.0138	-0.0110	
σ_z/q_1		0.5		3.3194	-0.0929	-0.6627	-0.7612	-0.4928	-0.0939
		0.4		2.3093	-0.2437	-0.7559	-0.8211	-0.5224	-0.1166
	0.3		1.4495	-0.3767	-0.8336	-0.8678	-0.5443	-0.1347	
	0.2		0.7061	-0.4961	-0.8997	-0.9045	-0.5604	-0.1493	
	0.2		0.8772	-0.4076	-0.8338	-0.8606	-0.5383	-0.1423	
	0.1		0.1480	-0.4972	-0.8471	-0.8439	-0.5212	-0.1470	
	0.0		-0.0652	-0.4937	-0.7636	-0.7413	-0.4533	-0.1292	
	-0.1		-0.0482	-0.4494	-0.6381	-0.6014	-0.3633	-0.1015	
	-0.2		0.0301	-0.3953	-0.5026	-0.4528	-0.2682	-0.0713	
	-0.3		0.0318	-0.3563	-0.3833	-0.3186	-0.1816	-0.0448	
	-0.4		-0.2195	-0.3647	-0.3138	-0.2286	-0.1212	-0.0297	
	-0.5		-1.0290	-0.4764	-0.3526	-0.2350	-0.1178	-0.0395	
	τ_{xz}/q_1	0.5		0.0314	0.0442	0.0616	0.0623	0.0619	-0.0182
		0.4		0.0262	-0.2049	-0.1308	-0.0461	0.0218	-0.0200
0.3			0.0202	-0.3981	-0.2820	-0.1331	-0.0130	-0.0202	
0.2			0.0134	-0.5413	-0.3959	-0.2007	-0.0428	-0.0189	
0.2			0.0336	-0.5129	-0.3564	-0.1608	-0.0031	-0.0306	
0.1			0.0163	-2.7282	-2.0419	-1.0841	-0.3079	-0.0643	
0.0			0.0000	-3.7616	-2.8356	-1.5264	-0.4649	-0.0750	
-0.1			-0.0135	-4.1539	-3.1434	-1.7047	-0.5376	-0.0747	
-0.2			-0.0236	-4.1161	-3.1241	-1.7037	-0.5511	-0.0678	
-0.3			-0.0304	-3.6375	-2.7694	-1.5190	-0.5041	-0.0541	
-0.4			-0.0346	-2.4793	-1.9001	-1.0550	-0.3686	-0.0285	
-0.5			-0.0383	-0.0539	-0.0751	-0.0759	-0.0754	0.0221	

On the other hand, although corresponding shapes of the displacement and stress distributions in the left part of corresponding clamped-free and clamped-guided beams are similar, they differ considerably when the right edge is approached. Moreover, the extent to which the stress boundary conditions imposed on the lateral planes of the beam are satisfied has remained essentially unchanged for the transverse shear stress, τ_{xz} , but it has slightly been improved for the transverse normal stress σ_z , at least away from the beam edges (Tables 6 and 8 and Figs 10, 13 and 14). Finally, in the case of the two-layered beam, the amount of discontinuity of the interlaminar stresses has slightly been increased on the clamped edge ($x = 0, z/h = 0.2$), but it can still be considered practically negligible everywhere else on the material interface (Table 8 and Fig. 13).

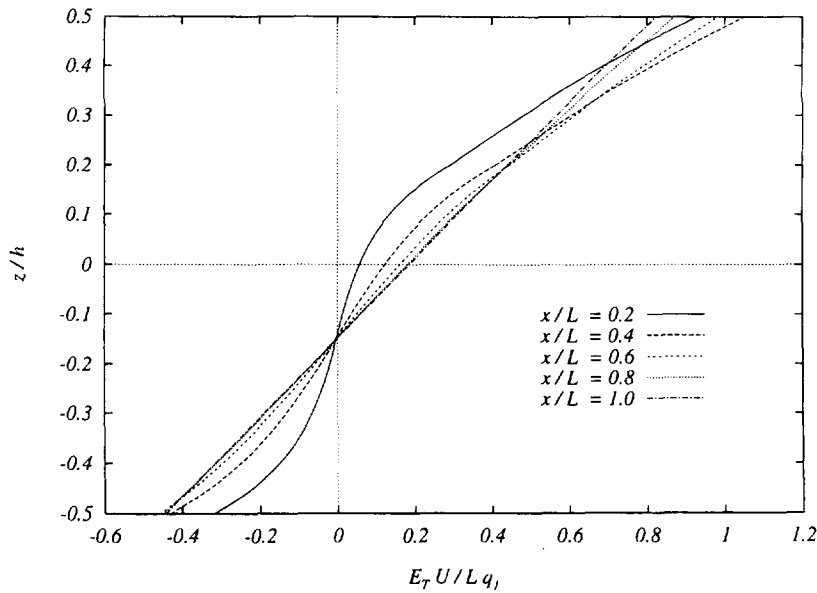


Fig. 5. In-plane displacement distributions for a clamped-free two-layered beam.

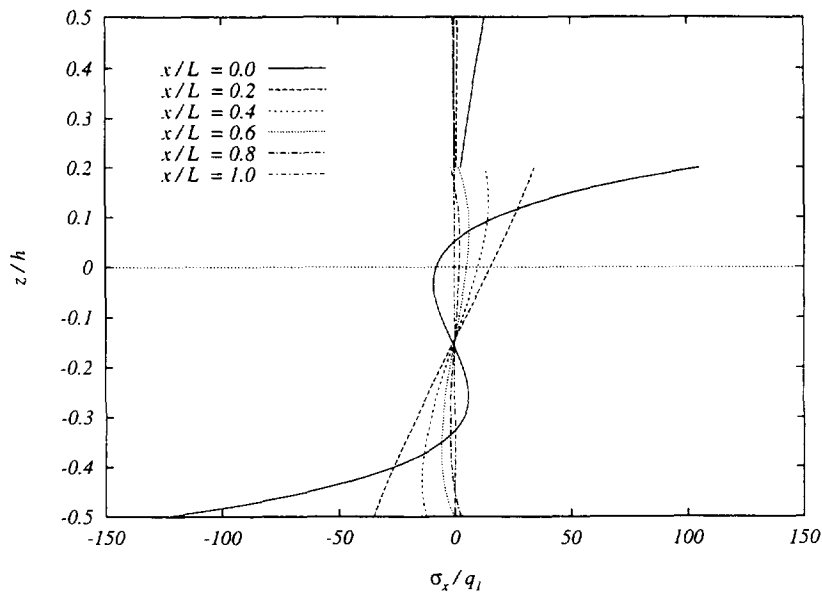


Fig. 6. Bending stress distributions for a clamped-free two-layered beam.

7. CONCLUSIONS

A method for improving the performance of one-dimensional, higher-order theories of homogeneous and laminated composite beams has been proposed in this paper. The method is based on the appropriate specification of through-thickness "shape functions" that are suitable for accurate stress analysis of beams, on the basis of a "general four-degrees-of-freedom" theory (G4DOFBT).

This new beam theory involves two shape functions, each of which is associated with one of the two unknown displacement components and, through them, it enables consideration of the effects of both transverse shear and transverse normal deformation. Further, it involves four unknown displacement functions (degrees of freedom), each one of which is assigned certain physical meaning. In particular applications, these are determined from the solution of four, one-dimensional, Navier-type equations of equilibrium, which form a tenth order set of simultaneous ordinary differential equations, with respect to the axial co-ordinate parameter, x .

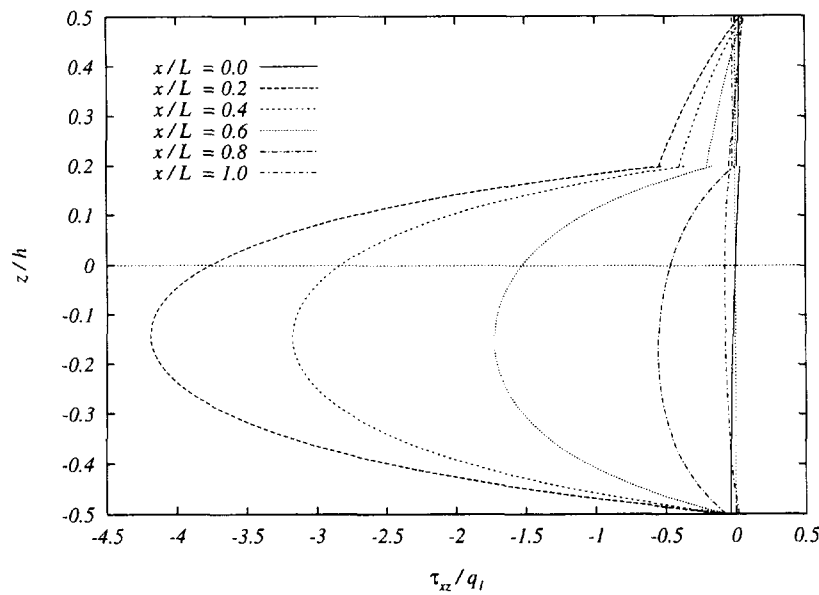


Fig. 7. Shear stress distributions for a clamped-free two-layered beam.

Table 5. Displacement distributions for a clamped-guided homogeneous beam

		x/L					
		0.0	0.2	0.4	0.6	0.8	1.0
$E_T U / L q_1$	0.5	0.0000	0.1752	0.1735	0.1233	0.0578	0.0000
	0.4	0.0000	0.0648	0.0823	0.0681	0.0368	0.0000
	0.3	0.0000	0.0163	0.0375	0.0380	0.0236	0.0000
	0.2	0.0000	-0.0017	0.0156	0.0204	0.0142	0.0000
	0.1	0.0000	-0.0052	0.0046	0.0086	0.0067	0.0000
	0.0	0.0000	-0.0028	-0.0020	-0.0008	0.0000	0.0000
	-0.1	0.0000	0.0000	-0.0083	-0.0101	-0.0067	0.0000
	-0.2	0.0000	-0.0022	-0.0184	-0.0214	-0.0141	0.0000
	-0.3	0.0000	-0.0174	-0.0382	-0.0379	-0.0231	0.0000
	-0.4	0.0000	-0.0601	-0.0787	-0.0657	-0.0356	0.0000
-0.5	0.0000	-0.1588	-0.1611	-0.1161	-0.0551	0.0000	
$E_T W / L q_1$	0.5	0.0000	-0.9632	-2.0704	-2.8227	-3.1601	-3.2079
	0.4	0.0000	-0.9487	-2.0498	-2.8027	-3.1482	-3.2058
	0.3	0.0000	-0.9346	-2.0297	-2.7831	-3.1365	-3.2037
	0.2	0.0000	-0.9218	-2.0114	-2.7653	-3.1259	-3.2018
	0.1	0.0000	-0.9107	-1.9957	-2.7500	-3.1168	-3.2002
	0.0	0.0000	-0.9017	-1.9828	-2.7375	-3.1093	-3.1988
	-0.1	0.0000	-0.8947	-1.9728	-2.7278	-3.1035	-3.1978
	-0.2	0.0000	-0.8896	-1.9656	-2.7208	-3.0993	-3.1970
	-0.3	0.0000	-0.8863	-1.9609	-2.7162	-3.0965	-3.1966
	-0.4	0.0000	-0.8843	-1.9580	-2.7134	-3.0949	-3.1963
-0.5	0.0000	-0.8825	-1.9555	-2.7110	-3.0934	-3.1960	

Introduction of the stress distributions, caused by the assumed G4DOFBT displacement model into the exact equations of plane strain elasticity has produced an excellent choice of both shape functions involved, as it led to the exact elasticity solution presented by Pagano (1969) for simply supported infinite strips. By means of those shape functions, exact through-thickness displacement and stress distributions are “extracted” from that well-known elasticity solution and are appropriately “fitted” into the corresponding distributions assumed for the development of G4DOFBT. Hence, the main physical characteristics of an exact elasticity solution are successfully incorporated into the proposed one-dimensional beam theory.

In more detail, any set of boundary conditions imposed on the lateral planes of a simply supported beam can be satisfied exactly. Moreover, in the case of laminated beams,

Table 6. Stress distributions for a clamped-guided homogeneous beam

		x/L						
		z/h	0.0	0.2	0.4	0.6	0.8	1.0
σ_x/q_1	0.5		102.6753	7.5100	-6.7156	-12.8803	-13.0037	-10.6674
	0.4		19.8375	7.4516	-0.4255	-5.3166	-7.2923	-7.5112
	0.3		-11.8043	6.1893	1.7811	-1.8698	-4.1552	-5.2133
	0.2		-18.2509	4.3343	1.9778	-0.4495	-2.2852	-3.3379
	0.1		-12.7017	2.1969	1.2171	0.0058	-1.0187	-1.6637
	0.0		-2.2568	-0.0559	0.0655	0.0668	0.0014	-0.0715
	-0.1		8.4775	-2.3159	-1.1097	1.0042	1.0066	1.5157
	-0.2		15.0487	-4.4783	-1.9531	0.4760	2.2210	3.1727
	-0.3		10.8958	-6.3887	-1.9416	1.7097	3.9744	5.0094
	-0.4		-15.9825	-7.7651	-0.1180	4.7705	6.8702	7.2271
	-0.5		-89.1215	-8.0543	5.3947	11.5506	12.0917	10.2204
σ_y/q_1	0.5		0.8556	-0.0870	-0.2691	-0.3146	-0.2321	-0.1110
	0.4		0.1653	-0.0929	-0.2243	-0.2590	-0.1889	-0.0855
	0.3		-0.0984	-0.0935	-0.1918	-0.2166	-0.1546	-0.0649
	0.2		-0.1521	-0.0917	-0.1657	-0.1809	-0.1248	-0.0467
	0.1		-0.1058	-0.0890	-0.1428	-0.1487	-0.0973	-0.0297
	0.0		-0.0188	-0.0861	-0.1215	-0.1181	-0.0708	-0.0132
	-0.1		0.0706	-0.0834	-0.1006	-0.0880	-0.0446	0.0032
	-0.2		0.1254	-0.0814	-0.0790	-0.0570	-0.0179	0.0199
	-0.3		0.0908	-0.0806	-0.0552	-0.0237	0.0105	0.0377
	-0.4		-0.1332	-0.0825	-0.0263	0.0152	0.0426	0.0576
	-0.5		-0.7427	-0.0895	0.0131	0.0653	0.0823	0.0819
σ_z/q_1	0.5		0.8556	-0.5359	-0.9086	-0.9365	-0.6034	-0.1773
	0.4		0.1653	-0.5578	-0.8866	-0.9031	-0.5734	-0.1541
	0.3		-0.0984	-0.5287	-0.8118	-0.8195	-0.5145	-0.1291
	0.2		-0.1521	-0.4753	-0.7122	-0.7123	-0.4420	-0.1033
	0.1		-0.1058	-0.4111	-0.6016	-0.5949	-0.3636	-0.0773
	0.0		-0.0188	-0.3431	-0.4876	-0.4741	-0.2834	-0.0512
	-0.1		0.0706	-0.2758	-0.3746	-0.3545	-0.2037	-0.0252
	-0.2		0.1254	-0.2135	-0.2672	-0.2401	-0.1272	0.0004
	-0.3		0.0908	-0.1627	-0.1722	-0.1374	-0.0574	0.0256
	-0.4		-0.1332	-0.1357	-0.1021	-0.0586	-0.0015	0.0497
	-0.5		-0.7427	-0.1565	-0.0824	-0.0276	0.0268	0.0720
τ_{xz}/q_1	0.5		-0.7435	0.1714	0.1511	0.1500	0.1486	0.0000
	0.4		-0.5689	-1.5349	-1.1335	-0.5616	-0.0974	0.0000
	0.3		-0.3979	-2.3703	-1.7650	-0.9192	-0.2325	0.0000
	0.2		-0.2429	-2.7694	-2.0689	-1.0980	-0.3095	0.0000
	0.1		-0.1094	-2.9440	-2.2039	-1.1834	-0.3544	0.0000
	0.0		0.0000	-2.9904	-2.2420	-1.2140	-0.3789	0.0000
	-0.1		0.0848	-2.9382	-2.2054	-1.2020	-0.3868	0.0000
	-0.2		0.1459	-2.7655	-2.0778	-1.1385	-0.3753	0.0000
	-0.3		0.1859	-2.3876	-1.7957	-0.9894	-0.3342	0.0000
	-0.4		0.2105	-1.6143	-1.2167	-0.6782	-0.2405	0.0000
	-0.5		0.2314	-0.0533	-0.0470	-0.0467	-0.0462	0.0000

continuity of both displacements and interlaminar stresses is satisfied at all material interfaces. The through-thickness distributions of in-plane displacement and stresses vary exponentially, and axial elastic moduli appear in the exponents. As these moduli may be assigned substantially high values in cases of highly reinforced materials, axial stress and displacement may accordingly take high values away from the central axis of a single layer, therefore giving rise to the well-known boundary layer behaviour of those stress and displacement distributions.

Implementation of these new types of shape function in the one-dimensional equations of G4DOFBT is not difficult to achieve, as shape functions enter G4DOFBT only by means of the constitutive eqns (10). As happens with all refined beam, plate and shell theories, any chosen set of shape functions influences only the values of the higher-order coupling and bending rigidities, by means of appropriate through-thickness integrations. Such integrations can easily be performed analytically but, if necessary, they may alternatively be

Table 7. Displacement distributions for a clamped-guided two-layered beam

		x/L					
		0.0	0.2	0.4	0.6	0.8	1.0
$E_T U/Lq_1$	0.5	0.0000	0.7650	0.7238	0.4939	0.2201	0.0000
	0.4	0.0000	0.5517	0.5402	0.3789	0.1744	0.0000
	0.3	0.0000	0.3671	0.3782	0.2756	0.1322	0.0000
	0.2	0.0000	0.2047	0.2330	0.1813	0.0928	0.0000
	0.2	0.0000	0.2047	0.2330	0.1813	0.0928	0.0000
	0.1	0.0000	0.0722	0.1103	0.0992	0.0570	0.0000
	0.0	0.0000	0.0190	0.0475	0.0492	0.0310	0.0000
	-0.1	0.0000	0.0013	0.0113	0.0136	0.0093	0.0000
	-0.2	0.0000	-0.0071	-0.0178	-0.0182	-0.0112	0.0000
	-0.3	0.0000	-0.0272	-0.0558	-0.0547	-0.0331	0.0000
	-0.4	0.0000	-0.0863	-0.1231	-0.1071	-0.0599	0.0000
-0.5	0.0000	-0.2311	-0.2551	-0.1942	-0.0972	0.0000	
$E_T W/Lq_1$	0.5	0.0000	-1.3590	-3.0537	-4.2747	-4.8790	-5.0010
	0.4	0.0000	-1.3484	-3.0385	-4.2608	-4.8715	-5.0008
	0.3	0.0000	-1.3360	-3.0209	-4.2446	-4.8627	-5.0007
	0.2	0.0000	-1.3222	-3.0012	-4.2266	-4.8529	-5.0005
	0.2	0.0000	-1.3222	-3.0012	-4.2266	-4.8529	-5.0005
	0.1	0.0000	-1.3080	-2.9811	-4.2081	-4.8428	-5.0003
	0.0	0.0000	-1.2947	-2.9621	-4.1906	-4.8333	-5.0001
	-0.1	0.0000	-1.2836	-2.9463	-4.1762	-4.8255	-5.0000
	-0.2	0.0000	-1.2754	-2.9345	-4.1654	-4.8196	-4.9999
	-0.3	0.0000	-1.2698	-2.9266	-4.1581	-4.8157	-4.9998
	-0.4	0.0000	-1.2664	-2.9217	-4.1536	-4.8132	-4.9998
-0.5	0.0000	-1.2634	-2.9174	-4.1497	-4.8111	-4.9997	

performed numerically, by using a standard numerical routine. This makes it clear, therefore, that as far as the accurate stress analysis of complicated material configurations is concerned (multi-layered beams), implementation of even more complicated forms of such shape functions is not regarded as a possible drawback of the proposed method.

For beams having both of their edges simply supported, the present formulation yields, naturally, the exact, plane strain, elasticity solution due to Pagano (1969). Hence, no numerical results were shown for simply supported plates as, in such a case, the present method will clearly yield results that are identical to those obtained by Pagano's (1969) exact elasticity analysis. Instead, only new results were presented and discussed in this paper and the efficiency of the method proposed has been exhibited with two examples dealing with the bending of homogeneous orthotropic and two-layered beams subjected to a certain sinusoidal loading.

These examples dealt with displacement and stress distributions within homogeneous orthotropic and two-layered cross-ply laminates which have one of their edges rigidly clamped and the other edge either free of tractions or guided. As was expected, away from the plate edges the displacement and stress distributions were dominated by the form of the shape functions employed. At the edges, however, these displacement and stress distributions were required to satisfy the edge boundary conditions imposed in a through-thickness averaged sense. In addition to this, it was shown that the present method was able to satisfy very accurately and in most cases exactly, that is in a three-dimensional point by point sense, the boundary conditions imposed on the plate edges. This is considered as a remarkable achievement of the proposed method, as it is essentially based on an one-dimensional beam theory. Nevertheless, the present approach enables a very systematic treatment of through-thickness averaged edge boundary conditions, as all possible combinations of variationally consistent sets have been expressed through eqns (12).

All results presented have shown that for the manner in which the proposed method was applied it was able to satisfy quite accurately, but not exactly, the stress boundary conditions imposed on the lateral planes of the beam, especially away from the beam edges. Although interlaminar stresses were predicted to be slightly discontinuous on a clamped edge, away from that edge they were practically, but again not exactly, continuous. This,

Table 8. Stress distributions for a clamped-guided two-layered beam

		x/L						
z/h		0.0	0.2	0.4	0.6	0.8	1.0	
σ_x/q_1	0.5	12.2940	0.5878	-1.0232	-1.5948	-1.4470	-1.0207	
	0.4	8.4239	0.4995	-0.7487	-1.2252	-1.1430	-0.8342	
	0.3	5.1492	0.4034	-0.5191	-0.9017	-0.8679	-0.6565	
	0.2	2.3361	0.3013	-0.3243	-0.6138	-0.6155	-0.4856	
	0.2	87.7390	16.9570	-4.1376	-15.6776	-19.1064	-18.1631	
	0.1	5.3583	13.1452	1.8938	-6.2344	-10.5291	-12.0850	
	0.0	-15.1850	8.0937	2.6499	-2.1344	-5.2808	-6.9281	
	-0.1	-8.1450	2.4890	1.0527	-0.4183	-1.5178	-2.1820	
	-0.2	6.2354	-3.2633	-1.1712	0.6632	1.8499	2.4548	
	-0.3	11.4462	-8.8320	-2.6134	2.5366	5.7110	7.2281	
	-0.4	-13.6723	-13.7931	-1.4688	7.0301	11.2045	12.4532	
	-0.5	-105.6730	-17.4140	5.3804	17.3020	20.2983	18.6745	
	σ_y/q_1	0.5	3.8479	0.0879	-0.4573	-0.6248	-0.5213	-0.3208
		0.4	2.6366	0.0404	-0.3996	-0.5351	-0.4402	-0.2626
0.3		1.6116	-0.0053	-0.3501	-0.4543	-0.3652	-0.2072	
0.2		0.7312	-0.0499	-0.3070	-0.3806	-0.2952	-0.1539	
0.2		0.7312	-0.0054	-0.2437	-0.3225	-0.2636	-0.1533	
0.1		0.0447	-0.0406	-0.1982	-0.2482	-0.1945	-0.1027	
0.0		-0.1265	-0.0641	-0.1655	-0.1898	-0.1376	-0.0595	
-0.1		-0.0679	-0.0828	-0.1388	-0.1388	-0.0863	-0.0196	
-0.2		0.0520	-0.1003	-0.1140	-0.0901	-0.0366	0.0195	
-0.3		0.0954	-0.1198	-0.0876	-0.0393	0.0147	0.0596	
-0.4		-0.1139	-0.1453	-0.0555	0.0189	0.0718	0.1034	
-0.5		-0.8806	-0.1839	-0.0104	0.0935	0.1416	0.1551	
σ_z/q_1		0.5	3.0976	-0.2364	-0.8060	-0.9046	-0.6380	-0.2623
		0.4	2.1225	-0.3379	-0.8497	-0.9150	-0.6177	-0.2164
	0.3	1.2974	-0.4248	-0.8813	-0.9155	-0.5930	-0.1724	
	0.2	0.5886	-0.5007	-0.9037	-0.9085	-0.5651	-0.1300	
	0.2	0.7312	-0.4456	-0.8712	-0.8981	-0.5766	-0.1592	
	0.1	0.0447	-0.4908	-0.8401	-0.8369	-0.5147	-0.1087	
	0.0	-0.1265	-0.4589	-0.7283	-0.7060	-0.4183	-0.0647	
	-0.1	-0.0679	-0.3933	-0.5815	-0.5449	-0.3071	-0.0237	
	-0.2	0.0520	-0.3196	-0.4266	-0.3768	-0.1925	0.0166	
	-0.3	0.0954	-0.2584	-0.2852	-0.2205	-0.0838	0.0578	
	-0.4	-0.1139	-0.2364	-0.1854	-0.1002	0.0070	0.1022	
	-0.5	-0.8806	-0.3001	-0.1761	-0.0584	0.0590	0.1536	
	τ_{xz}/q_1	0.5	0.0916	0.0446	0.0616	0.0623	0.0617	0.0000
		0.4	0.0765	-0.2046	-0.1308	-0.0461	0.0218	0.0000
0.3		0.0588	-0.3979	-0.2820	-0.1331	-0.0128	0.0000	
0.2		0.0392	-0.5411	-0.3959	-0.2007	-0.0425	0.0000	
0.2		0.0979	-0.5125	-0.3564	-0.1608	-0.0029	0.0000	
0.1		0.0475	-2.7278	-2.0419	-1.0841	-0.3061	0.0000	
0.0		0.0000	-3.7613	-2.8356	-1.5264	-0.4623	0.0000	
-0.1		-0.0394	-4.1536	-3.1434	-1.7046	-0.5347	0.0000	
-0.2		-0.0689	-4.1160	-3.1241	-1.7036	-0.5482	0.0000	
-0.3		-0.0887	-3.6375	-2.7694	-1.5189	-0.5015	0.0000	
-0.4		-0.1010	-2.4795	-1.9001	-1.0549	-0.3667	0.0000	
-0.5		-0.1116	-0.0543	-0.0751	-0.0759	-0.0752	0.0000	

however, cannot be considered as a serious disadvantage of the present method, mainly because the values of transverse stresses are at least one order of magnitude lower than the values of the bending stresses, the distributions of which are considered to be extremely accurate. Moreover, with the method being based on what is essentially a one-dimensional laminate beam theory, a remarkable credibility should be recognised for the vast majority if not for all of the numerical results presented and discussed.

Nevertheless, a procedure to possibly improve, or even entirely eliminate, the effects of this slight inaccuracy has been outlined and discussed in Section 5. This would require the solution of a highly non-linear system of simultaneous algebraic equations, the number of which depends on the number of the layers in a particular laminate. Such a laborious and numerically complicated procedure was not employed in the present study, mostly

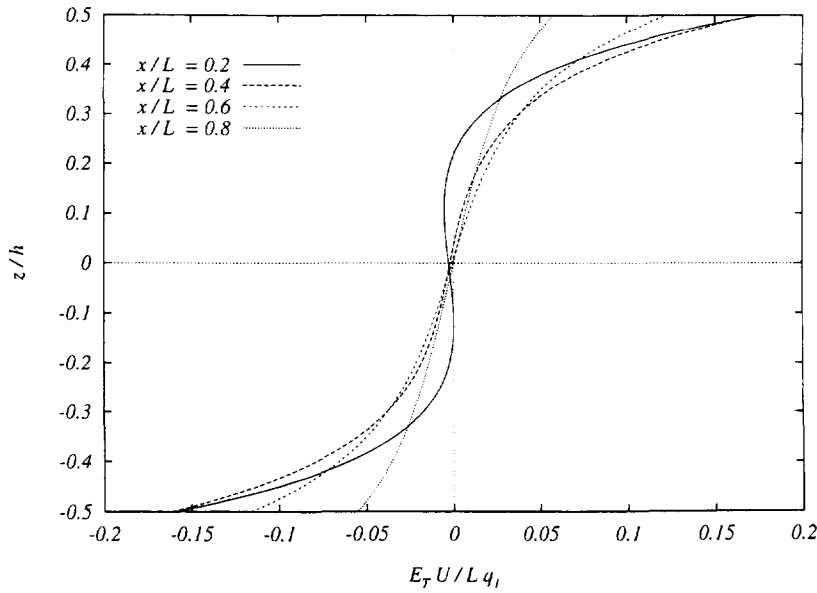


Fig. 8. In-plane displacement distributions for a clamped-guided homogeneous beam.

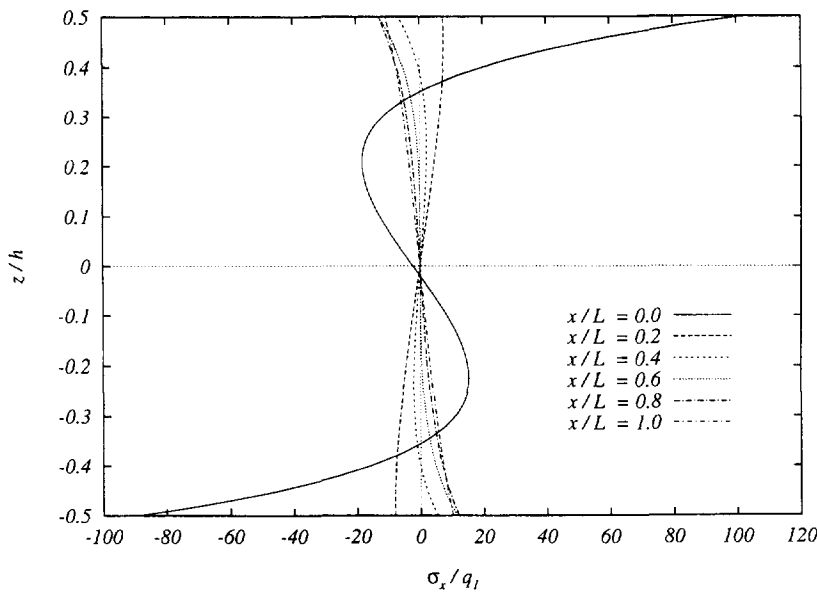


Fig. 9. Bending stress distributions for a clamped-guided homogeneous beam.

because it is currently uncertain whether its possible success will be found to have any practical importance. The possibility, however, has been left open for a future extension of the present method towards this direction.

It should be finally noted that, at its present form, the proposed model has been outlined and is therefore only available in connection with geometrically linearly elastic problems. The possibility, however, of extending its applicability for the accurate stress analysis of beams subjected geometrically non-linear deformations is wide open. The easiest way to do so is by superimposing, onto the linear equations of G4DOFBT, the well-known von Karman type non-linearities which, however, are entirely consistent only with the assumptions of the classical plate and beam theories. An alternative way, which fits better with the assumptions of the G4DOFBT but the equations involved are more complicated, is described in Soldatos (1993b) and is consistent with shear deformable plate and beam theories for laminated composites.

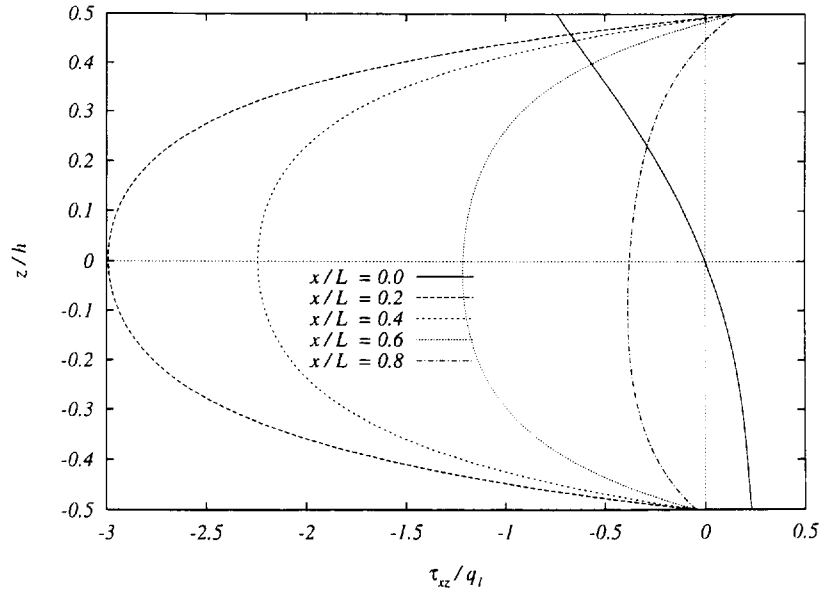


Fig. 10. Shear stress distributions for a clamped-guided homogeneous beam.

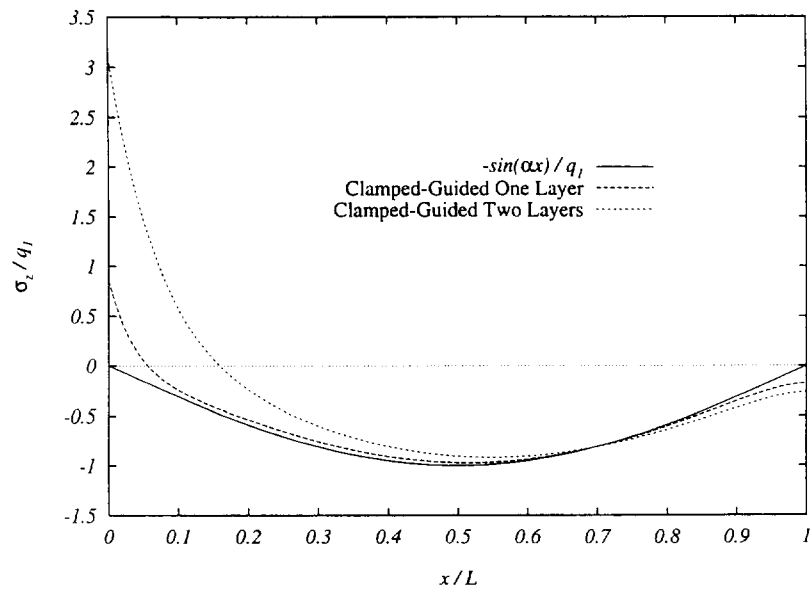


Fig. 11. Fit of transverse normal stress at upper lateral surface for clamped-guided beams.

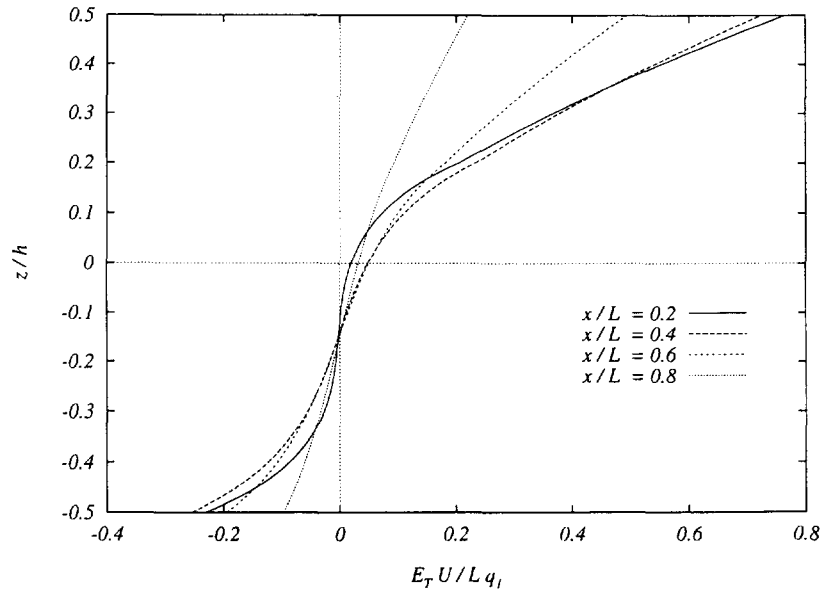


Fig. 12. In-plane displacement distributions for a clamped-guided two-layered beam.

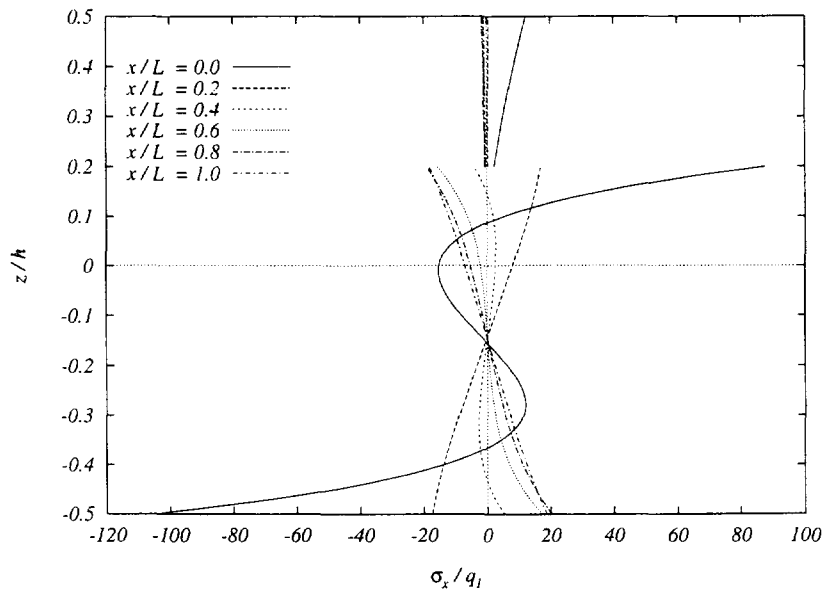


Fig. 13. Bending stress distributions for a clamped-guided two-layered beam.

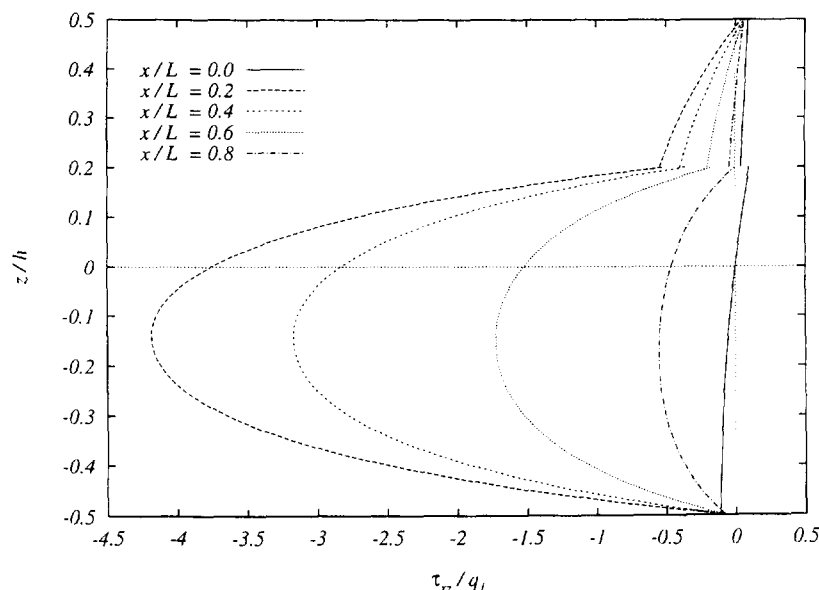


Fig. 14. Shear stress distributions for a clamped-guided two-layered beam.

Acknowledgements—The work described in this paper was supported by the EPSRC Research Grant No. GR/H42680.

REFERENCES

- Bickford, W. B. (1982). A consistent higher-order beam theory. *Developments in Theoretical and Applied Mechanics* **11**, 137–142.
- Cho, M. and Parmerter, R. R. (1992). An efficient higher-order plate theory for laminated composites. *Computers & Structures* **20**, 113–123.
- Di Sciuva, M. (1986). Bending, vibration and buckling of simply supported thick multilayered orthotropic plates: an evaluation of a new displacement model. *Journal of Sound and Vibration* **105**, 425–442.
- Di Taranto, R. A. (1973). Static analysis of a laminated beam. *Journal of Engineering in Industry* **95**, 755–761.
- Donnell, L. H. (1976). *Beams, Plates and Shells*, McGraw-Hill, New York.
- Heuer, R. (1992). Static and dynamic analysis of transversely isotropic, moderately thick sandwich beams by analogy. *Acta Mechanica* **91**, 1–9.
- Jones, R. M. (1975). *Mechanics of Composite Materials*, Hemisphere, New York.
- Pagano, N. J. (1969). Exact solution for composite laminates in cylindrical bending. *Journal of Composite Materials* **3**, 398–411.
- Rao, D. K. (1976). Static response of stiff-cored unsymmetric sandwich beams. *Journal of Engineering in Industry* **98**, 391–396.
- Rao, D. K. (1977). Vibration of short sandwich beams. *Journal of Sound and Vibration* **52**, 253–263.
- Rao, D. K. (1978). Frequencies and loss factors of multicore sandwich beams. *Journal of Mechanics Design* **100**, 667–674.
- Savithri, S. and Varadan, T. K. (1990). Free vibration and stability of cross-ply laminated plates. *Journal of Sound and Vibration* **141**, 516–520.
- Soldatos, K. P. (1992a). A transverse shear deformation theory for homogeneous monoclinic plates. *Acta Mechanica* **94**, 195–220.
- Soldatos, K. P. (1992b). A general laminated plate theory accounting for continuity of displacements and transverse shear stresses at material interfaces. *Computers & Structures* **20**, 195–211.
- Soldatos, K. P. (1992c). A four-degrees-of-freedom cylindrical shell theory accounting for both transverse shear and transverse normal deformation. *Journal of Sound and Vibration* **159**, 533–539.
- Soldatos, K. P. (1993a). Vectorial approach for the formulation of variationally consistent higher-order plate theories. *Computers in Engineering* **3**, 3–17.
- Soldatos, K. P. (1993b). A non-linear transverse shear deformable plate theory allowing a multiple choice of trial displacement and stress distributions. *Computers in Engineering* **3**, 885–897.
- Soldatos, K. P. (1995). Generalization of variationally consistent plate theories on the basis of a vectorial formulation. *Journal of Sound and Vibration* **183**, 819–839.
- Soldatos, K. P. and Timarci, T. (1993). A unified formulation of laminated composite shear deformable five-degrees-of-freedom cylindrical shell theories. *Computers & Structures* **25**, 165–171.
- Srinivas, S. and Rao, A. K. (1970). Bending, vibration and buckling of simply supported thick orthotropic rectangular plates and laminates. *International Journal of Solids and Structures* **6**, 1463–1481.
- Timoshenko, S. (1922). On the transverse vibrations of bars of uniform cross-section. *Philosophical Magazine* **43**, 125–131.
- Touratier, M. (1992). A refined theory of laminated shallow shells. *International Journal of Solids and Structures* **29**, 1401–1415.

Ye, J. Q. and Soldatos, K. P. (1994a). Three-dimensional vibrations of laminated cylinders and cylindrical panels with a symmetric or an antisymmetric cross-ply lay-up. *Computers in Engineering* **4**, 429–444.
 Ye, J. Q. and Soldatos, K. P. (1994b). Three-dimensional stress analysis of orthotropic and cross-ply laminated hollow cylinders and cylindrical panels. *Computational Methods in Applied Mechanics and Engineering* **117**, 331–351.

APPENDIX

For the case of a clamped-free beam, the non-zero elements of the matrix **M** in eqn (30) are given as follows ($i = 1, 2, 3, 4$):

$$\begin{aligned}
 M_{1,i} &= \frac{1}{\mu_i} [A_{55}^{aa} F_1 F_5 + \mu_i^2 (F_3 G_2 - F_5 G_1)], \quad M_{1,8} = 1, \\
 M_{2,i} &= \frac{1}{\mu_i^2} [A_{55}^{aa} F_1 F_4 + \mu_i^2 (F_2 G_2 + F_4 G_1)], \quad M_{2,10} = 1, \\
 M_{3,i} &= \frac{1}{\mu_i} [A_{55}^{aa} F_1 F_4 + \mu_i^2 (F_2 G_2 - F_4 G_1)], \quad M_{3,9} = 1, \\
 M_{4,i} &= \mu_i G_2, \quad M_{4,6} = \frac{F_2 G_4 - F_4 G_2}{A_{55}^{aa} F_1 G_4}, \\
 M_{5,i} &= (A_{55}^{aa} F_1 - \mu_i^2 G_1), \quad M_{5,5} = \frac{F_5}{G_4}, \quad M_{5,7} = -\frac{F_4}{G_4}, \\
 M_{6,5} &= 1, \\
 M_{7,6} &= 1, \\
 M_{8,6} &= L, \quad M_{8,7} = 1, \\
 M_{9,i} &= [A_{55}^{aa} (G_2 + A_{55}^{ab} F_1) - \mu_i^2 A_{55}^{ab} G_1] e^{\mu_i L}, \quad M_{9,5} = \frac{F_5 (G_2 + A_{55}^{ab} F_1) - F_3 G_4}{F_1 G_4}, \\
 M_{9,6} &= -\frac{F_4 (G_2 + A_{55}^{ab} F_1) - F_2 G_4}{F_1 G_4} L, \quad M_{9,6} = -\frac{F_4 (G_2 + A_{55}^{ab} F_1) - F_2 G_4}{F_1 G_4}, \\
 M_{10,i} &= \mu_i (A_{55}^{aa} A_{55}^{bb} F_1 + A_{55}^{ab} G_2 - \mu_i^2 A_{55}^{bb} G_1) e^{\mu_i L}, \quad M_{10,6} = \frac{A_{55}^{ab} (F_2 G_4 - F_4 G_2) - A_{55}^{aa} A_{55}^{bb} F_1 F_4}{A_{55}^{aa} F_1 G_4}, \quad (A1)
 \end{aligned}$$

and the corresponding vector **B** is given by,

$$\mathbf{B} = - \left[F_1 \tilde{A} \quad 0 \quad \alpha F_1 \tilde{C} \quad \tilde{B} \quad 0 \quad 0 \quad -\frac{(-1)^m q_m}{\alpha} \quad 0 \quad 0 \quad (-1)^m (A_{55}^{ab} \tilde{B} + \alpha A_{55}^{bb} \tilde{D}) \right]^T. \quad (A2)$$

When the edge $x = L$ is guided, only the sixth, eighth and ninth rows are changed in matrix **M** and their non-zero elements are given as follows:

$$\begin{aligned}
 M_{6,i} &= \frac{1}{\mu_i} [A_{55}^{aa} F_1 F_5 + \mu_i^2 (F_3 G_2 - F_5 G_1)] e^{\mu_i L}, \quad M_{6,5} = Q_2 L, \\
 M_{6,6} &= -\frac{1}{2} Q_2 L^2, \quad M_{6,7} = -Q_2 L, \quad M_{6,8} = 1, \\
 M_{8,i} &= \frac{1}{\mu_i} [A_{55}^{aa} F_1 F_4 + \mu_i^2 (F_2 G_2 - F_4 G_1)] e^{\mu_i L}, \quad M_{8,5} = Q_2 L, \\
 M_{8,6} &= -\frac{1}{2} Q_1 L^2, \quad M_{8,7} = -Q_1 L, \quad M_{8,9} = 1, \\
 M_{9,i} &= \mu_i G_2 e^{\mu_i L}, \quad M_{9,6} = \frac{F_2 G_4 - F_4 G_2}{A_{55}^{aa} F_1 G_4}, \quad (A3)
 \end{aligned}$$

and the corresponding vector **B** is now given by,

$$\mathbf{B} = - \left[F_1 \tilde{A} \quad 0 \quad \alpha F_1 \tilde{C} \quad \tilde{B} \quad 0 \quad (-1)^m F_1 \tilde{A} \quad -\frac{(-1)^m a_m}{\alpha} \quad \alpha (-1)^m F_1 \tilde{C} \quad (-1)^m \tilde{B} \quad (-1)^m (A_{55}^{ab} \tilde{B} + \alpha A_{55}^{bb} \tilde{D}) \right]^T. \quad (A4)$$